People's Democratic Republic of Algeria
Ministry of Higher Education and Scientific Research

University M'Hamed BOUGARA – Boumerdes

Institute of Electrical and Electronic Engineering

Department of Power and Control

Final Year Project Report Presented in Partial Fulfilment of
the Requirements for the Degree of

MASTER

In **Electrical and Electronic Engineering**

Option: **Control/Power Engineering**

Title:

PV Module Parameters Identification Using Global Search Algorithms

Presented by:

- **AGOUDJIL Mohamed Abdellah**
- **BOUREDJI Khalid**

Supervisor:

Dr. KHELDOUN Aissa

Registration Number:………/2017

Abstract

The nonlinear behavior of photovoltaic modules (PV) and their dependence on the working conditions imply a reliable forecasting of its behavior at different temperatures and irradiance. It is therefore essential with the growing demand of this technology to develop effective methods for accurate extraction of the module intrinsic parameters.

This project presents a novel approach to extract automatically and accurately the photovoltaic module single-diode model five parameters I_{ph}, I_{sat}, A, R_s, and R_p using the obtained Data from the acquisition circuit. The main contribution of this project is the use of different algorithms with different PV modules in order to extract highly accurate results. Six algorithms are used to estimate the five parameters of ten modules. The local algorithm uses "fsolve" to solve resulting nonlinear equations, while the six other global algorithms use their global search feature to extract parameters and draw the I-V curve.

Dedication

I dedicate this effort to Mom, who bought me hundreds of books.

To Dad who believed in me more than his jokes.

To my brother who was my companion through many long nights.

To my lovely sister with whom I had some lovely fights.

To the memory of my grandparents who loved me and thought me handsome.

To all my family and friends who helped me and made me a better person.

Khalid BOUREDJI

Dedication

I would like to dedicate this work to my soul and my heart, my mother.

To the person that I admire the most in this world, my father.

To my sister who always supported me.

To the memory of my grandparents who taught me the importance of hard work.

To my teacher who made me believe that humility is one of the most important quality a human being should have.

To J K Rowling who was present in the long journey.

To my friends who guided me when I needed answers, who impacted my life with their positive energy and showed me that obstacles are made to be broken.

To my colleague, Khalid who believed in me since the first day.

Mohamed Abdellah AGOUDJIL

Acknowledgment

We would first like to thank our thesis advisor Dr. Kheldoun of the Institute of Electrical and Electronic Engineering at University of Boumerdes. The door to Dr. Kheldoun office was always open whenever we ran into a trouble spot or had a question about our research or writing.

We would also like to extend our thanks to all IGEE teachers and staff for the knowledge and the guidance they provided us throughout our academic journey in the institute.

Finally, we must express our very profound gratitude to our parents and friends for providing us with unfailing support and continuous encouragement throughout our years of study and through the process of researching and writing this thesis. This accomplishment would not have been possible without them.

Table of Contents

List of Tables

List of Figures

List of Abbreviations and Acronyms

PV: Photovoltaic.

DC: Direct Current.

AC: Alternating Current.

STC: Standard Test Conditions.

AM: Air Mass.

MPP: Maximum Power Point.

I_{ph}: Photocurrent.

I_d: P-N junction current.

Ip: Current that passes through the parallel resistance of a PV cell.

R_s: Series resistance in the equivalent circuit of a PV cell.

R_p: Parallel resistance in the equivalent circuit of a PV cell.

I_{sat}: Diode saturation current.

A: The diode ideality factor.

FF: Fill Factor.

V_{oc}: Open Circuit Voltage.

I_{sc}: Short Circuit Current.

I_{mpp}: Maximum Power Point Current.

V_{mpp}: Maximum Power Point Voltage.

V_t: The thermal voltage.

I-V curve: Current versus voltage curve.

P-V curve: Power versus voltage curve.

N_s: Number of series PV cells.

N_p: Number of parallel PV cells.

NRMSE: Normalized Root Mean Square.

FA Algorithm: Firefly Algorithm.

DE Algorithm: Differential Evolution Algorithm.

PSO Algorithm: Particle Swarm Optimization Algorithm.

EM Algorithm: Exchange Market Algorithm.

BA: Bees Algorithm.

General Introduction

General introduction

Adding to the fact that conventional energy sources are harmful to the global climate, the high rate of consumption of fossil fuels could run them out by the early twenty-second century. This implies that humanity will heavily rely on renewable sources of energy, which explains the growing interest and focus of research on sustainable energy development, among which solar electric generation which has the highest power density among renewable energies.

Solar power provides energy reliability as sun is present as a permanent and stable source of energy. This energy source has also been identified as a nonpolluting solution for the pressing issue of global warming. Further, the fact that PV installation can operate for 30 years or even more with little maintenance reduces its operating costs and makes it insignificant comparing to existing power technologies. Solar power is provided after the conversion of light into electricity by means of semiconducting materials that exhibit the photovoltaic effect. This conversion is done at the level of a basic elementary device of PV system which is the PV cell.

However, the performance of photovoltaic systems is entirely dependent on the working condition they are established in. The electrical output is subject to variations due to the fluctuating temperature and irradiance that depend on the season and location conditions. Consequently, researchers worked on developing suitable models for photovoltaic (PV) cells and modules to simulate and forecast their behavior under different circumstances, which is central to the design, manufacturing, and evaluation of PV systems. Also, an accurate estimation of the models' parameters is at the heart of the reliability of each model. For this project, our interest is on the extraction of the five parameters of single-diode model. Through this work, we contribute to the design of a PV panels parameters identification card by focusing on the use of global search algorithms in our parameters extraction.

This project is organized as follow: The first chapter is an overall background photovoltaic system principle and construction, and also the importance of PV panel parameters and the challenges facing this technology. The second chapter covers the modeling and simulation of the PV panel model and describes the data acquisition circuit. The third chapter deals with the methods to extract the cell's single-diode model intrinsic five parameters. The chapter presents six algorithms: one local and five global. These algorithms are adapted to our search of the five parameters with the least possible error. It compares the results and select the best algorithms to be used in the card to analyze the behavior of a photovoltaic system.

Chapter One

Photovoltaic System Principles

1.1 Introduction

Solar energy is one of the important and abundant source of renewable energy, and many scientists believe that the sun is the source that will permit to ensure a greener future for the planet. Solar energy has a lot of advantages, it is a free energy that can be transformed to electricity by means of photovoltaic panels and it reduces air pollution. However, it also has some disadvantages which are presented at the end of this chapter.

In the first chapter a general overview about the solar energy will be given. We will introduce the principle of photovoltaic and explain how a photovoltaic cell works. The characteristics and the parameters of the solar cell will be presented, as well as the conventional models used to study the PV panels.

The parameters of the solar cell are responsible of the performance of the photovoltaic system. This is why we will focus in this project on the practical ways used in order to determine the parameters of a photovoltaic panel.

1.2 Photovoltaic

Photovoltaic is a word composed of photo which means light and voltaic which stands for voltage. Photovoltaics (abbreviated PV) is the most direct way to convert solar radiation into electricity. Photovoltaic or solar cells are semiconductor devices that transform sunlight into direct current (DC) electricity. PV cells are arranged in modules and arrays, and can be used to charge batteries, operate motors and to power any number of electronics loads; from small electronics like calculators up to homes. PV systems are also able to produce alternating current (AC) if they are equipped with the power conversion equipment, inverters.

1.3 Photovoltaic Cells

1.3.1 Structure

Photovoltaic cells are made of two or more thin layers of semi-conducting material, generally silicon. They don’t contain any moving parts and don’t use any fluids. When exposed to solar radiation the semiconductor generates electrical charges which can be conducted away by metal contacts as direct current (DC). Photovoltaic cells are the safest and the most environmentally friendly energy production, because they do not pollute and produce no noise.

Technologies have allowed us to create several types of photovoltaic cells:

- Monocrystalline silicon PV panels

These are made using cells sliced from a single crystal of silicon. This is the most energetic photovoltaic technology, typically converting around 15% of the sun's energy into electricity. The manufacturing process required to produce monocrystalline silicon is complicated, resulting in slightly higher costs than other technologies. [1]

- Polycrystalline silicon PV panels

Known also as multi-crystalline cells, polycrystalline silicon cells are made from cells cut from an ingot of melted and recrystallized silicon. They are generally cheaper to produce than monocrystalline cells, but they are lightly less efficient. Their efficiency is around 12%. [1]

- Amorphous silicon PV panels

Amorphous silicon cells are made by depositing silicon in a thin homogenous layer onto a substrate rather than creating a rigid crystal structure. This technology is less efficient than crystalline silicon, with typical efficiencies of around 6%, but it tends to be easier and cheaper to produce. [1]

1.3.2 Photovoltaic Effect

A solar cell is a large-area semiconductor diode. It consists of a P-N junction created by an impurity addition (doping) into the semiconductor crystal. The N-region of the crystal is doped with phosphorus-atoms, and the P-region with boron atoms. Due to the doping, it is known that the N-region contains a lot of free electrons. In the other hand the P-region have a lack of them, and each missing electron can be seen as a “hole” so this region has more free holes than free electrons. Due to the differences in concentration at the junction between the two regions, electrons diffuse into the p-regions and “holes” into n-regions, therefore an electrical field in the formerly electrical neutral junction comes into existence. [2]

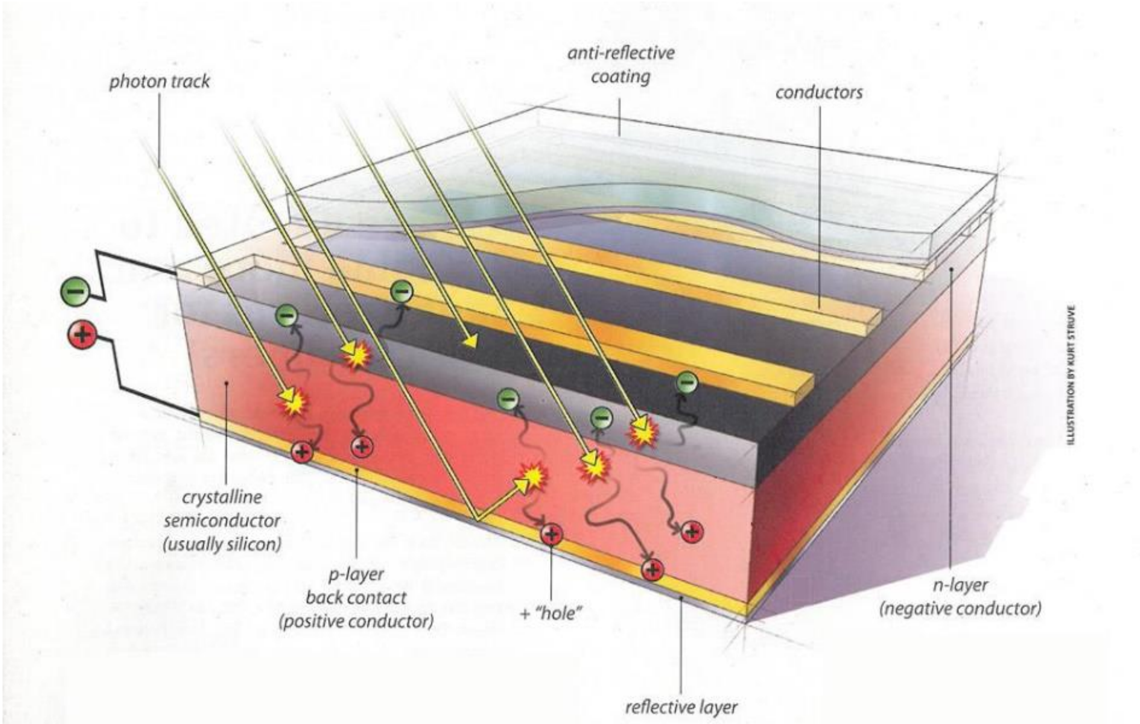

Figure 1.1: Diagram of a typical crystalline silicon solar cell [3]

Photons falling on the PN junction cause the rise of pairs of opposite electrical charge carriers (electron – hole), which as a result of the presence of PN junction are separated in two different directions. Electrons go to the semiconductor N and holes go to the semiconductor P. The voltage will arise on the junction. Because the separated electrical charges are redundant carriers, having so called, infinite life and a PN junction voltage is constant, the junction, on which the light falls acts as a stable electric cell. The current (and power) output of a PV cell depends on its efficiency and size (surface area), and is proportional to the intensity of sunlight striking the surface of the cell. A typical silicon PV cell produces about 0.5 – 0.6 v DC under open-circuit, no-load conditions, which is not sufficient to charge batteries or run motors. In order to generates enough voltages PV cells are connected in series and the result are called PV modules. [2] [4]

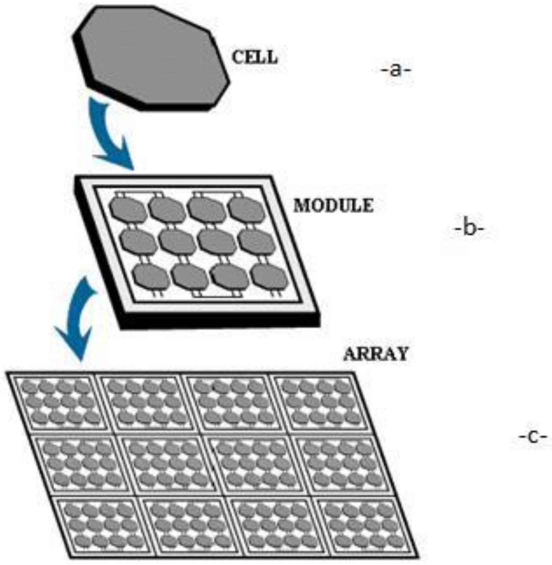

Figure 1.2: a) cell b) module c) array [5]

1.3.3 The Electrical Characteristics of a PV Cell

Electrical characteristics of PV modules are given by the producers under precise conditions, which are known standard test conditions (STC). Such conditions are defined by the cell temperature T_{STC} = 25°C, irradiation level G_{STC} = 1000 W/m^2, and the air mass value, this measure represents the effect of the air mass between a surface and the sun on the spectral distribution and intensity of sunlight, AM = 1.5.

The current vs voltage characteristics of a PV panel working under uniform conditions are described by the following curves.

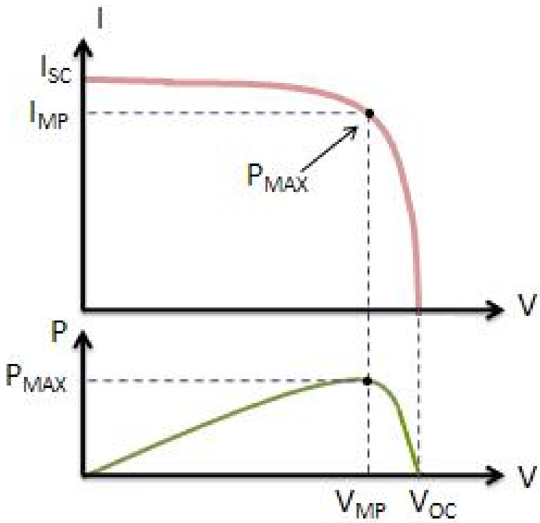

Figure 1.3: current versus voltage curve [6]

A Current (I) versus Voltage (V) Curve of a PV module shows the possible combinations of its current and voltage outputs. The power in a DC electrical circuit is the product of the voltage and the current.

$$P\ (\text{Watts}) = I\ (\text{Amperes}) \times V\ (\text{Volts}) \tag{1.1}$$

A solar panel generates its maximum current when there is no resistance in the circuit, in other words; when there is a short circuit between its Positive two terminals (positive and negative). This maximum current is known as the Short Circuit Current and is abbreviated as I_{sc}. When the panel is shorted, the voltage in the circuit is zero.

In the other hand, the maximum voltage is obtained when there is a break in the circuit. This is called the Open Circuit Voltage (V_{oc}). In this situation, the resistance is infinitely high and the current is equal to zero, since the circuit is deficient. Typical value of the open-circuit voltage is located about 0.5 and 0.6 V for Crystalline Cells and between 0.6 and 0.9 V for Amorphous Cells. The I_{sc} and V_{oc} occurs at the two extremes of the load resistance. These two points and the whole range of conditions in between them, are characterized on the I-V Curve. Current is represented on the vertical axis and the voltage on the horizontal axis. They are expressed in amps and volts respectively.

The power produced from a photovoltaic panel can be calculated at any point along the I-V curve. It consists of the product of the current in and the voltage at that point and is expressed in Watts. The power output is equal to zero at both, the short circuit current point, and the open circuit voltage point, the power output is also zero. The maximum power output is obtained on the knee of the I-V Curve where and this point is called the Maximum Power Point (MPP). The voltage and current at this Maximum Power Point are designated as V_{mpp} and I_{mpp}. [6]

So, in order to model a PV cell, three important points are needed:

- Point one corresponds to the maximum current the solar cell can provide the solar cell at the zero voltage (short circuit current).
- Point two corresponds to the maximum voltage of the solar cell without a charge (open circuit condition)
- Point three corresponds to the maximum power that can be generated by the solar cell.

1.3.4 PV Cell Modelling

From the I-V curves discussed before we can deduce the equivalent circuit for a PV cell to represent the high nonlinearity that results from the semiconductor junction which is the basis of its realisation. Two models of the PV cell are presented: Single-diode and the double-diode models.

A) Single Diode Model

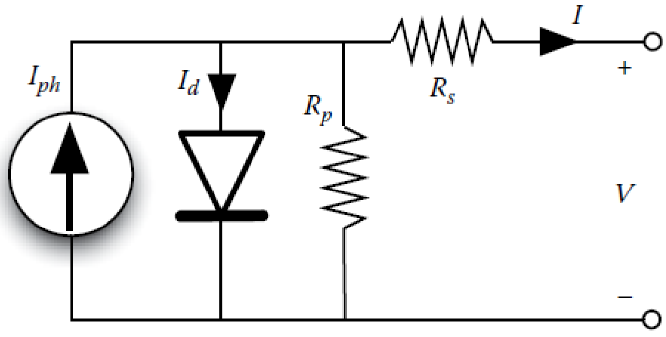

Figure 1.4: Single diode model for PV cell [7]

The above circuit is equivalent to a single diode-model of a photovoltaic cell. It consists of current source with a parallel diode and a network of resistors. Where the diode takes speaks for the physical effects taking place at the silicon p-n junction of the cell. The current generator represents the photo-induced current, which is dependent on the characteristics of the semiconductor used to build up the cell, and especially, the area of the cell, irradiation level, and temperature. The series resistance represents the intrinsic resistance of the semiconductor, the resistance of the metal grid connecting individual PV cells in a panel, as well as the connection resistance and the connecting cable resistance. In the other hand the parallel resistance illustrate the inherent shunt of a PV module.

This circuit is governed by the following equation: [7]

$$I = I_{ph} - I_D - I_p \tag{1.2}$$

In this model, the I_D is modelled using the Schockley equation for an ideal diode

$$I_D = I_{sat}\,(e^{\frac{V+I\,R_S}{n\,V_t}} - 1) \tag{1.3}$$

Where I_{sat} is the saturation current, n is the ideality factor of the diode, usually between 1 and 2, and V_t is the thermal voltage given by the following equation:

$$V_t = \frac{k\ T}{q} \tag{1.4}$$

Where k is Boltzmann's constant (1.381×10^{-23} J/k), q is the electron charge (1.602×10^{-19} C)

Note that the saturation current can be computed by

$$I_{sat} = C\,T^3\,e^{(\frac{-E_{gap}}{k\,T})} \tag{1.5}$$

Where E_{gap} is the band gap of the semiconductor material and C is the temperature coefficient.

Writing the shunt current as

$$I_p = \frac{V+I\,R_S}{R_p} \tag{1.6}$$

When we combine all the above equations we obtain the overall equation that governs this model: [7]

$$I = I_{ph} - I_{sat}\left(e^{\frac{V+I\,R_S}{n*V_t}} - 1\right) - \frac{V+I\,R_S}{R_p} \tag{1.7}$$

B) Double Diode Model

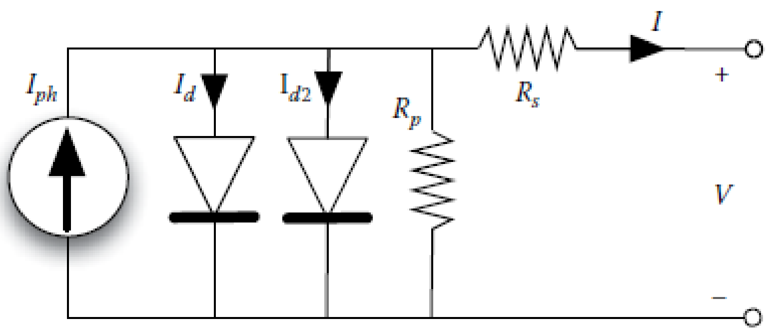

Figure 1.5: Double diode model for PV cell [7]

This is the modified form of single diode circuit which takes into account the effect of recombination that takes place in the space-charge zone by introducing another diode in parallel. Due to this new model, the current versus voltage characteristic equation will be defined by the following equation: [7]

$$I = I_{ph} - I_{sat}\left(e^{\frac{V+I\,R_S}{n\,V_t}} - 1\right) - I_{sat2}\left(e^{\frac{V+I\,R_S}{n_2\,V_t}} - 1\right) - \frac{V+I\,R_S}{R_p} \tag{1.8}$$

Where the second saturation current is described by: [7]

$$I_{sat2} = C_2\, T^{\frac{5}{2}}\, e^{(\frac{-E gap}{2\, k\, T})} \tag{1.9}$$

For simplicity purpose the single diode model is chosen to identify the parameters of the photovoltaic cell.

1.4 PV Cell Parameters and Their Effect

1.4.1 Fill Factor

The short-circuit current and the open-circuit voltage are the maximum current and voltage that can be obtained respectively from a photovoltaic cell. However, at both of these operating points, the power generated by the solar cell is equal to zero. The "fill factor", abbreviated "FF", is a parameter used to express the maximum power produced by a solar cell in terms of V_{oc} and I_{sc}, The FF is defined as the ratio of the maximum power from the solar cell to the product of V_{oc} and I_{sc}. FF can also be interpreted graphically as the ratio of the rectangular areas depicted in the following figure. [8]

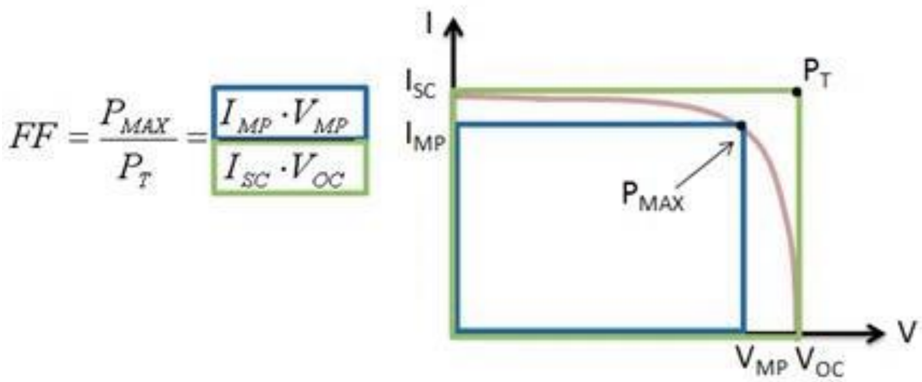

Figure 1.6: Graph of the I-V curve representing the power points [9]

In the illustration above we can see clearly the short circuit current and open circuit voltage points, along with the maximum power point, and the maximum theoretical power (P_T).

The more commonly used expression for FF is:

$$FF = \frac{V_{oc} + \ln(V_{oc} + 0.72)}{V_{oc} + 1} \tag{1.10}$$

The fill factor is directly affected by the values of the cell's series, shunt resistances and diodes losses. Increasing the parallel resistance (R_p) and decreasing the series resistance

(R_s) lead to a higher fill factor, thus resulting in greater efficiency, and bringing the cell's output power closer to its theoretical maximum. The reason for which the fill factor is calculated by comparing the maximum power to the theoretical power (PT) that would be output at both the open circuit voltage and short circuit current together.

$$FF = \frac{I_{mpp}\ V_{mpp}}{I_{sc}\ V_{oc}} \tag{1.11}$$

1.4.2 Efficiency

The efficiency is the most commonly used parameter to compare the performance of different solar cells. Efficiency is defined as the ratio of the output power, P_{out}, from the solar cell, compared to the solar power input, P_{in}, into the PV cell. P_{out} can be taken as P_{max} since the PV cell can operate up to its maximum power. P_{in} is considered as the product of the irradiance of the incident light with the surface area of the solar cell. [9]

In addition to reflecting the performance of the solar cell itself, the efficiency depends on the spectrum and intensity of the incident sunlight and the temperature of the solar cell. Therefore, conditions under which efficiency is measured must be carefully controlled in order to compare the performance of one device to another. This is done under STC conditions. The efficiency is computed using the following equation:

$$n = \frac{V_{oc}\ I_{sc}\ FF}{P_{in}} \tag{1.12}$$

1.4.3 Effect of Parallel Resistance

The parallel resistance or the shunt resistance used in our model lead to a significant power loses, due to manufacturing defects. Low shunt resistance causes power losses in PV cells by providing an alternate current path for the light-generated current. This diversion decreases the amount of current that passes through the PV cell junction, this phenomenon is illustrated by the equation 1.2. It also, reduces the voltage generated by the solar cell. The impact of the parallel resistance is particularly noticed at low light levels, because the light-generated current will be smaller. The loss of this current to the shunt therefore has a larger impact. Moreover, the effect of the shunt resistance is more serious at lower voltages where the effective resistance of the solar cell is higher. [8]

1.4.4 Effect of Series Resistance

The series resistance of our model will lead to a movement of current through the emitter and base of the solar cell, besides it will create a contact resistance between the metal contact and the silicon. The series resistance will also cause the resistance of the top and rear metal contacts.

The series resistance does not affect the solar cell at the open circuit voltage and is considered to be zero because the current flow through the solar cell. In the other hand the series resistance affect the I-V curve near the short circuit current and it also decreases the fill factor. [8]

1.5 Effect of Temperature

Sun's radiations are composed of light and heat. Temperature has no effect on the amount of solar energy that reaches the PV panel. However, it reduces the amount of energy converted into electrical energy. When temperature increases the band gap of the semiconductor material will be reduced, this will also have an impact on the semiconductor parameters.

The decrease in the band gap plus the increasing temperature will increase the energy of the electrons. So, less energy is required in order to take them from a lower energy state to a higher energy state. The decrease in the potential difference between the excited electrons and the electrons at rest will produce a slightly smaller amount of power.

In a solar cell, the parameter most affected by an increase in temperature is the open-circuit voltage.

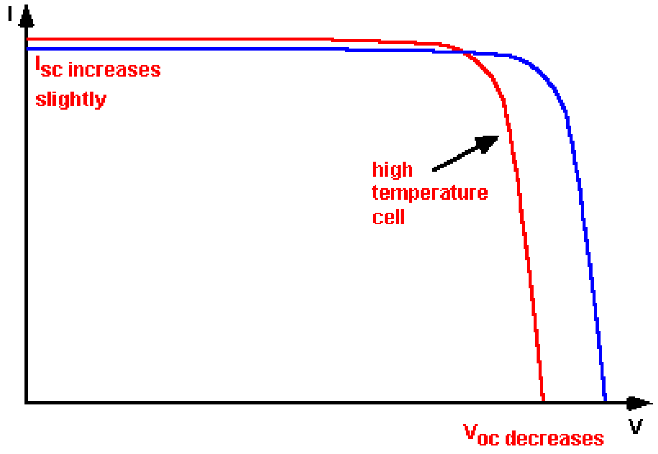

Figure 1.7: Effect of the temperature on the I-V curve [8]

1.6 Effect of Light Intensity

Light intensity has a huge impact on the PV cell parameters, a small variation in light intensity will change the short circuit current, the open circuit voltage, the fill factor, the efficiency, and the impact of both the series and shunt resistances. The standard test light intensity is 1 kW/m^2 or AM 1.5.

Solar cells are subject to daily variations in light intensity. At low light levels, the effect of the shunt resistance becomes more important. When light intensity decreases, the current in the PV cell also decreases, and its equivalent resistance approaches the value of the shunt resistance. When these two are equal, the amount of the current flowing through the shunt resistance increases, this increases the fractional power loss due to the shunt resistance. From this we can conclude that in a cloudy day, a solar cell shunt resistance retains a greater fraction of its original power than a solar cell with a low shunt resistance.

1.7 Identification of PV Cell Parameters

We have presented the current versus voltage relationship of the single diode PV cell model and we noticed that the equation of the I-V curve was nonlinear, which is difficult to solve by the analytical methods

Due to this difficulty scientists have developed several algorithms in order to solve this equation to determine the parameters of the solar cell. These algorithms are divided into two main categories:

- **Local algorithms**

The local algorithms are used to solve the current-voltage equation of a single diode model of a photovoltaic cell and to determine its 5 parameters, I_D, I_{ph}, R_p, R_s, and n, based on the datasheets provided by the manufacturers and initial guess solution. However, the output results of these algorithms are not exact.

- **Global algorithms**

Like the local algorithms, the global algorithms were developed in order to estimate the solar cell parameters. However, these algorithms are based on identification methods that extract the needed data from a single I-V curve. Unlike the local algorithms, the global ones do not need initial guess and they provide more accurate results because of their ability to find and use the global optima of the cost function instead of the local optima.

1.8 Advantages of Solar Energy

Solar energy is non-polluting, clean, reliable and renewable source of energy. It does not realise toxic gases that pollute the air like carbon dioxide, nitrogen oxide or sulphur oxide. So, the risk of damage to the environment is reduced. Solar energy is used to produce electricity as long as the sun exists, it does not require any fuel, thus avoids problems related to fuel transportation and storage of radioactive waste. This energy is transformed to electricity by means of solar panels that can reduce our dependence on fossil fuels. It is also considered to be an interesting prospect for countries that are aiming to go completely green in the next decades.

One of the most interesting things about solar energy is that it can be used at home by installing PV panels. They are easy to install and do not require any wires, cords or power sources. The cost of installing the solar panels may be high. However, when it is running the user will enjoy its benefits because they make no noise at all and there are no moving parts in solar cells which makes them long lasting and require very little maintenance.

1.9 Obstacles Facing the Development and Use of Solar Energy

Although the various advantages provided by the use of solar energy, we should point out that this energy has also some disadvantages. Here is an outline of basic disadvantages of solar energy: [10][11]

1.9.1 Reliability

Unlike the other sources of renewable energy, solar panels do not generate energy at night or in cloudy days. Which means that the user will be dependent on the local utility grid to draw power when the sun is not shining. Another solution is to invest in battery backup systems, which store up power to be used when there is no sun.

1.9.2 Initial Cost

Although installation of solar panels would bring immense benefits, the initial cost of the installation is high. This is due to the demand and supply curve. As the demand for solar energy increases, the cost would also decrease in time. However, since the energy generated after installation is absolutely free, in the long run, the user will be able to recover his invested money.

1.9.3 Pollution

Although pollution related to solar energy systems is far less compared to other sources of energy, solar energy can be associated with pollution. The PV panels are made of some hazardous products and toxic materials, which can directly affect the environment. Their transportation and installation have been source of greenhouse gases. A solar cell has a lifespan of about half a century, disposing of these materials can have serious impacts on the environment. This is a challenge that we have to deal with in the future years. Nevertheless, solar energy pollutes far less than the other alternative energy sources.

1.9.4 Efficiency

Another obstacle facing solar energy is photovoltaic efficiency. Efficiency is all about the amount of space it takes to generate the energy. In the desert, a single square meter of solar panel could receive the equivalent of more than 6 KWh of energy in one single day. But the PV panel is not able to convert all that energy to electricity. The efficiency of a solar panel determines how much of that power is usable, and most commercial solar panels on the market have efficiency ratings of less than 25 percent. The more efficient a panel is, the more expensive it is.

1.9.5 Shading

One of the most important step before designing solar power system is to investigate a location for the solar installation platform where the PV panels will be located. For a maximum of power all the panels have to be exposed to light without any shading that may be caused by surroundings buildings, trees, objects or vegetation. A 10% shading of a solar array can lead to a 50% decline in efficiency and on certain occasion to a total system shutdown. This is due to the way cells are connected within solar panels and the centralized form of performance optimization, carried out by the array inverter. Most solar arrays are made from panels connected in a series of parallel "strings." Each one of them provide the inverter with DC current, which will be converted into AC, while also optimizing the power generation. In the same time, each panel is composed of series connected cells. To prevent the whole string of cells from failing in case one of underperformance of one of them, the typical installation is equipped with "bypass diodes." These reroute the current around the underperforming cells. This mechanism will lead to a loss in the potential energy from these cells and also a decrease in the entire string's voltage.

In this situation, the inverter will maximize the energy harvest from the unaffected strings which will lead to a drop in the output energy of the impaired string. [12]

1.10 Conclusion

Solar energy is a renewable energy that can be transformed to electricity by means of photovoltaic panels. Even if this process presents some disadvantages in particular cases, solar energy offers more advantages than the traditional sources of energy (oil, coal …) and is considered to be the most important source for the future of our planet.

In this chapter, we presented the theoretical process of the transformation of solar energy and the different parameters of the photovoltaic panel and their effect on the output power.

We have also discussed the principle of efficiency and its dependence on many external conditions (temperature, light intensity …) and parameters.

The photovoltaic cell is modeled by mean of equivalent circuits in order to determine its parameters. Some of this circuits where presented in this chapter: The single diode model and the double diode model. Mathematical relationships between current and voltage were derived from this circuits. However, these equations were difficult to solve because of their nonlinearity. For this reason, scientists have developed local and global algorithms to identify the needed parameters.

In the following chapters, we will present and simulate the single diode model of a solar cell and show how global algorithms are used in order to determine the values of the different parameters of our model.

Chapter Two

Modeling and Data Acquisition of a PV Module

2.1 Introduction

Prototyping is an important step for any project because it permits to the developer to have an insight about the problems that he may face when realising his final product. This is why this chapter will be dedicated to the modelling and simulation of the single diode model of a PV panel.

The first step will be to simulate our PV panel using the appropriate software and to obtain the current versus voltage curve that helps us in the next chapter in order to obtain the five parameters of our model. In the second part of this chapter an implementation of our prototype is performed based on the circuit and steps presented in the final year project “PV Module Parameters Identification using Datasheet and Experimental Data”, 2016. In the last part of this chapter our system will be tasted in different weather conditions in order to illustrate the effect of the obstacles that may face the use of PV panels.

2.2 Modelling

Proteus 8 professional will be used in order to build the needed circuit to display the variation of the current versus the voltage (the I-V curve):

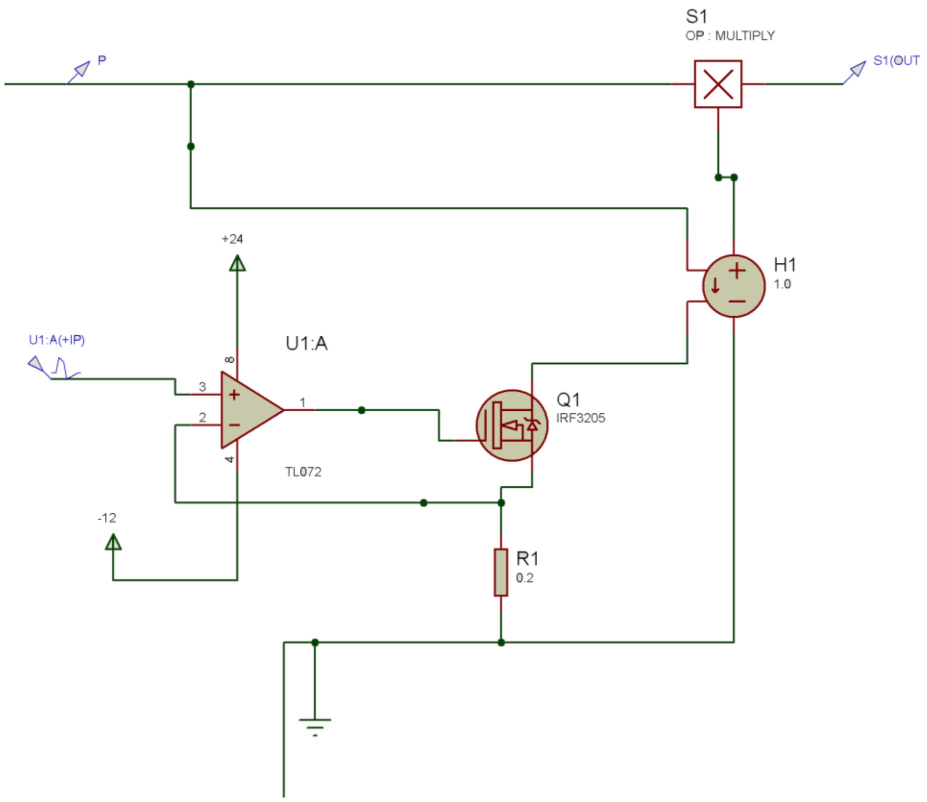

Figure 2.1: The IV curve drawer circuit

In this project, the solar cell is modelled as a single diode model.

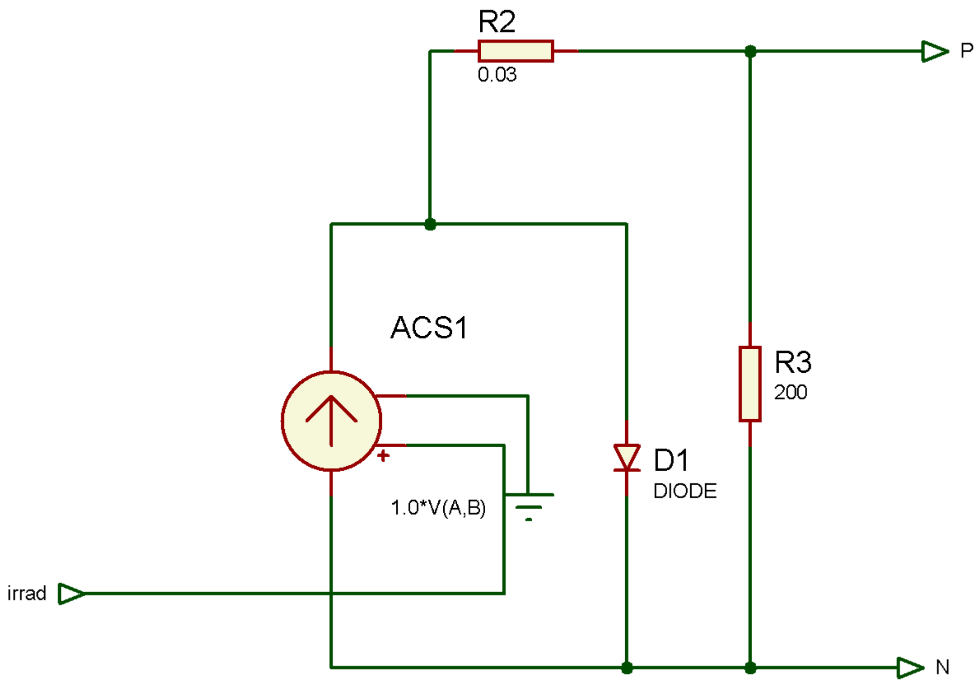

Figure 2.2: The solar cell model

The circuit used to build I-V curve is supplied by a circuit of identical cells. Each cell has one input (irrad) that simulates light irradiance and two outputs that represent the DC output with its terminals: positive and negative. In order to simulate a PV module, 16 PV cells are connected in series as shown in the following circuit. 8 cells are connected with one irradiance input and the remaining with a second irradiance input in order to model the shading effect that we have discussed in the previous chapter.

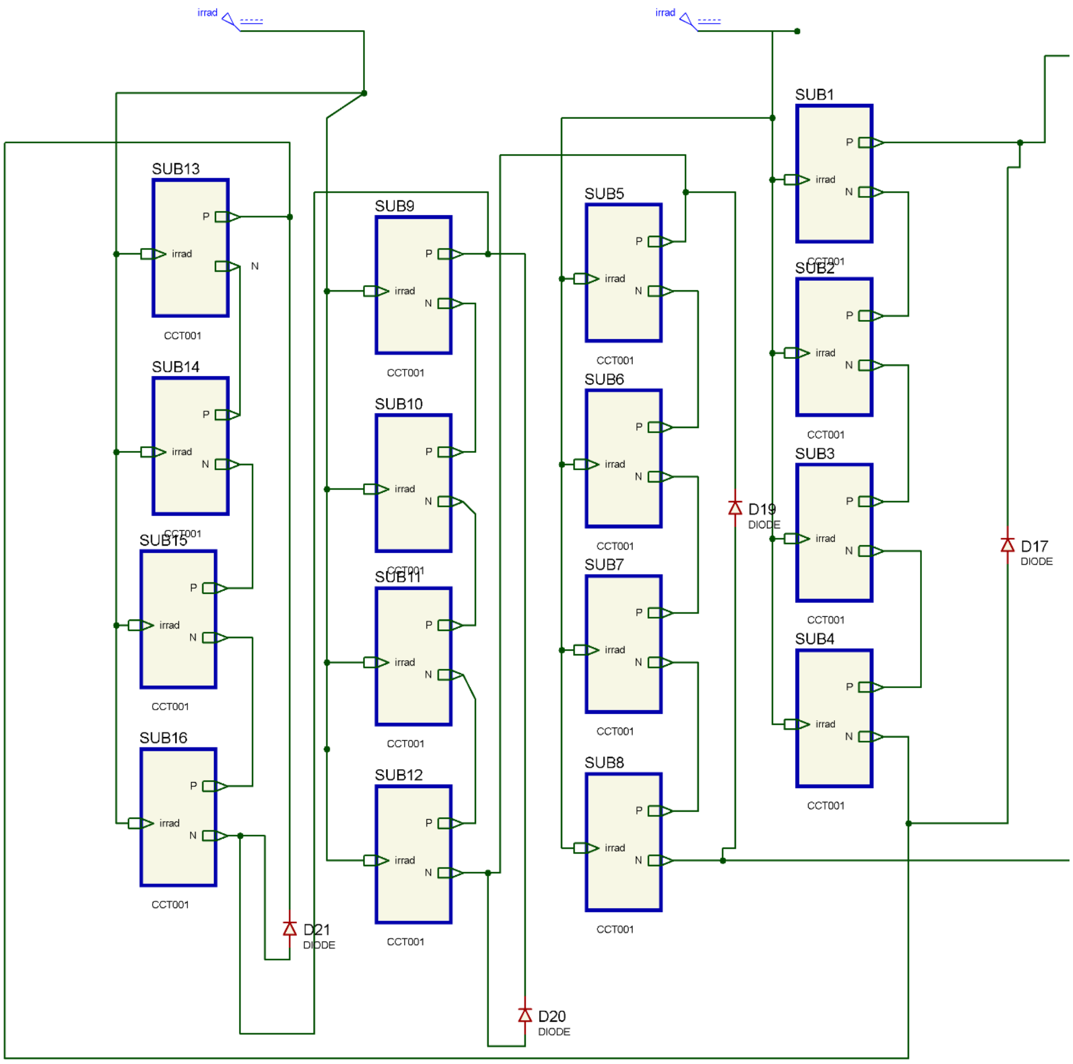

Figure 2.3: The PV panel model

Bypass diodes were used in this circuit in order to prevent the string of cells from failing in case of an underperformance of one of them during partial shading.

The whole circuit used to model the PV panel and to plot the current versus voltage curve is shown in Figure 2.4.

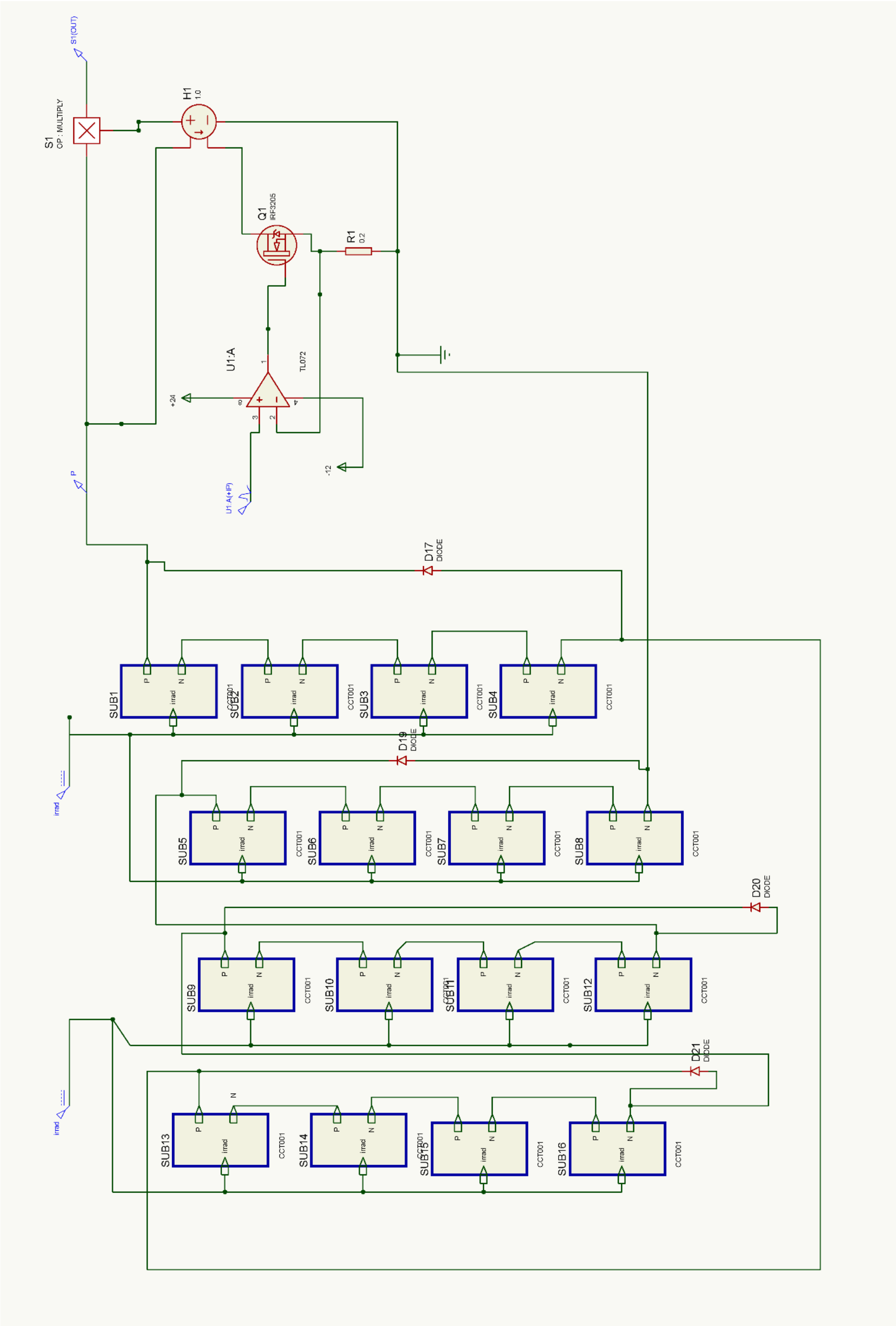

Figure 2.4: The PV panel modelling system used to obtain the I-V curve

2.2.1 Operation Principle

In the previous circuit, a MOSFET has been connected to the photovoltaic panel; the positive terminal to the drain and the negative terminal to the source. The current flowing to the gate is governed by a ramp input to an operational amplifier. The voltage coming from the photovoltaic panel is limited by the gate currents and it depends on the ramp value. The obtained results of the current and voltage will allow us to derive the I-V curve, including its main points $(0, I_{sc})$, $(V_{oc}, 0)$, and (V_{mpp}, I_{mpp}). Multiplying the voltage output by its corresponding current will allow us to sketch the power versus voltage curve [13].

2.3 Simulation

In this project, it is considered that the cells of the PV module have the same characteristics, and that they are subject to the same conditions of temperature and irradiance.

For the same current values of the two irradiance inputs we obtain the following I-V and P-V curves:

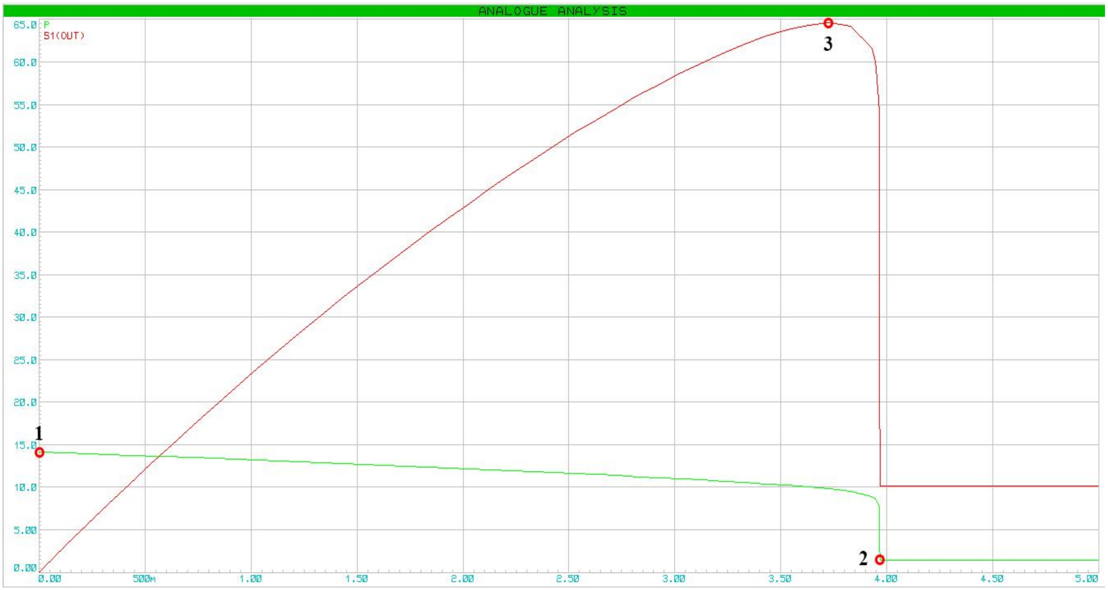

Figure 2.5: Power and current versus voltage curves

In the previous figure the red curve represents the power versus voltage curve whereas the green one represents the current versus voltage curve. The previous curve show also the three "conspicuous" points of the I-V characteristic curve. These points are the short circuit point $(0, I_{sc})$ represented by the point number (1), the open circuit point $(V_{oc}, 0)$ (2) and the maximum power point (V_{mpp}, I_{mpp}) (3).

2.3.1 Shading Effect

The shading effect is one of the obstacles that may face the use of PV panels, it may be caused by surrounding buildings, trees, objects, clouds or birds. The shading effect is simulated in our project by the use of different values of irradiance inputs. The results are shown in the figures 2.6 and 2.7.

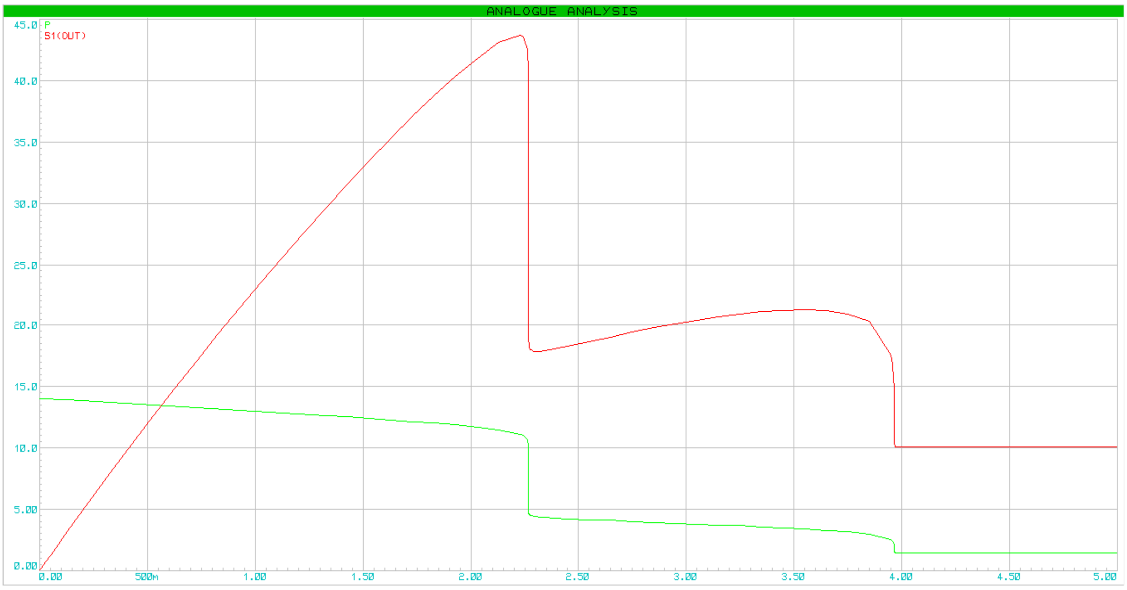

Figure 2.6: Power and current versus voltage curves with shading phenomena 1

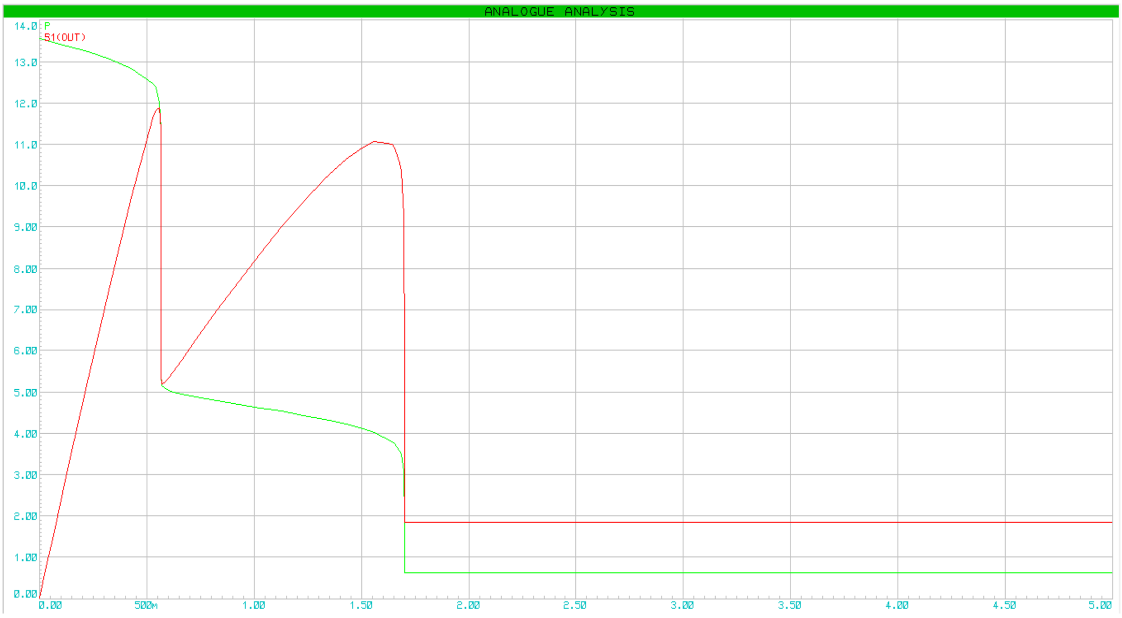

Figure 2.7: Power and current versus voltage curves with shading phenomena 2

2.4 Data Acquisition Circuit Implementation

The simulated circuit used previously in order to obtain the current versus voltage curve is implemented in order to identify the parameters of the photovoltaic panel.

The Arduino Due is used as an interface between the hardware and the software parts.

The block diagram of our system is shown in the following figure.

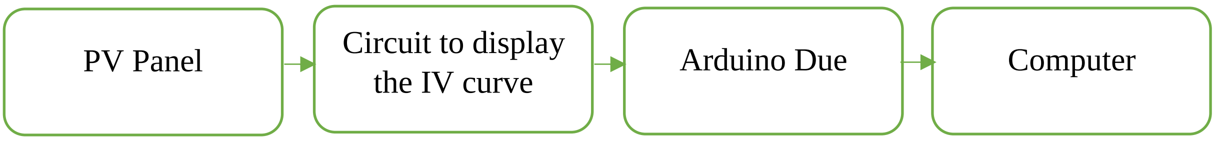

Figure 2.8: Schematic diagram of our system

2.4.1 Components and Material

In order to implement our circuit the following components are used:

- Resistors (used as voltage divider)
- Power resistors
- potentiometer
- Operational amplifier (LM358P)
- MOSFET (BUK 555)
- Regulators (MC7812AC & LM340AT-12)
- Single-Phase transformer
- Capacitors
- Diodes
- STP050D-12/MEA PV Panel with the characteristics presented in Table 2.1

Table 2.1: Characteristics of the STP050D-12/MEA PV Panel

Open circuit voltage(V)	**Optimum operating voltage(V)**	**Short circuit current(A)**	**Optimum operating current(A)**	**Maximum power STC (W_p)**	**Operating temperature (°C)**
21.8	17.4	3.13	2.93	50	-40°C to +80°C

2.4.2 Arduino Due

Arduino board designs use a variety of microprocessors and controllers. The boards are equipped with sets of digital and analog input/output (I/O) pins that may be interfaced to various expansion boards (shields) and other circuits. The boards feature serial communications interfaces, including Universal Serial Bus (USB) on some models, which are also used for loading programs from personal computers. The microcontrollers are typically programmed using a dialect of features from the programming languages C and C++. In addition to using traditional compiler toolchains, the Arduino project provides an integrated development environment (IDE) based on the Processing language project. [14]

In this project, an Arduino Due will be used. The Arduino Due is based on the Atmel SAM3X8E ARM Cortex-M3 CPU. It is the first Arduino board based on a 32-bit ARM core microcontroller. It has 54 digital input/output pins (of which 12 can be used as PWM outputs), 12 analog inputs, 4 UARTs (hardware serial ports), an 84 MHz clock, an USB OTG capable connection, 2 DAC (digital to analog), 2 TWI, a power jack, an SPI header, a JTAG header, a reset button and an erase button. [15]

The ramp used to control the output current of the PV panel is generated using the DAC of the Arduino board.

The analog inputs of the Arduino Due A0 and A1 will send the current an voltage trough the serial port to the software.

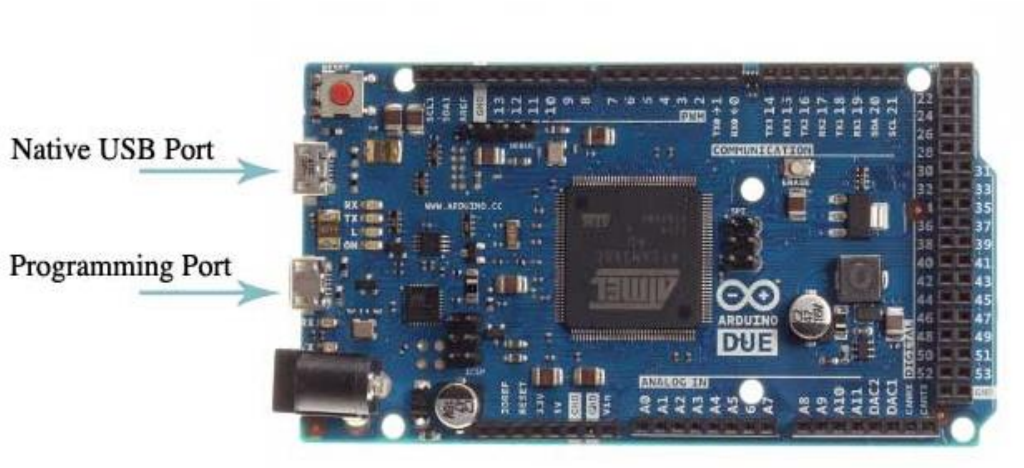

Figure 2.9: The Arduino Due [15]

2.4.3 Softwares

2.4.3.1 Arduino IDE 1.6.8:

It is an open source Arduino software that allows us to write code and upload it to the board. The code can be written in java and based on processing and other open source software.

2.4.3.2 MATLAB:

MATLAB (matrix laboratory) is a high-level programming language developed by MathWorks. MATLAB is a numerical computing environment that allows users to perform matrix manipulations, plot functions and data, and implement different algorithms. It also permits the creation of user interfaces, and interfacing with programs written in other programming languages.

2.4.4 Software Procedure

2.4.4.1 Arduino

The Arduino dur board is programmed using the Arduino IDE 1.6.8 by following these procedure: [13]

- The analog inputs A0 and A1 are set for the voltage and current respectively.
- We use the function “analog.write” (DAC0) to generate the needed ramp to plot the I-V curve.
- The serial library “serial.print” is used to allow the reception of the incoming serial data (current and voltage) through the USB port.

2.4.4.2 MATLAB

A MATLAB script is used in order to receive the data from the Arduino and save them. The script follows these steps: [13]

- set a variable s => to receive the serial data from the COM port.
- Let serial “BaudRate” same as the one in the Arduino IDE.
- open(s).
- Receive the string of data.
- Convert the obtained string to an [I V] array.
- Save your result using the “diary” option.

2.4.5 Operation Principle of the Circuit

- The positive terminal of the PV panel is connected to the drain of the MOSFET. Whilst the negative terminal is grounded.
- The gate of the MOSFET is connected to the output of the operational amplifier.
- The ramp (out of the DAC0) is connected first to the potentiometer to control the current following to the positive input of the operational amplifier. The ramp governs the current following to the gate and influences the I-V curve generated by the PV panel.
- The current that passes through the power resistances does not exceed the range of current tolerated by the Arduino board. The voltage that results from the voltage divider fall also within the accepted range. The results of the experiment are then sent to the analog inputs of the Arduino board. The current to the input A1, while the voltage to A0.
- The serial communication included in the program uploaded to the Arduino board and the used MATLAB script, help the user to receive the sampled data obtained during the experiment. [13]

2.4.6 Results and Discussion

The experiment has been completed first in a sunny day and the obtained results are shown in the figure 2.10

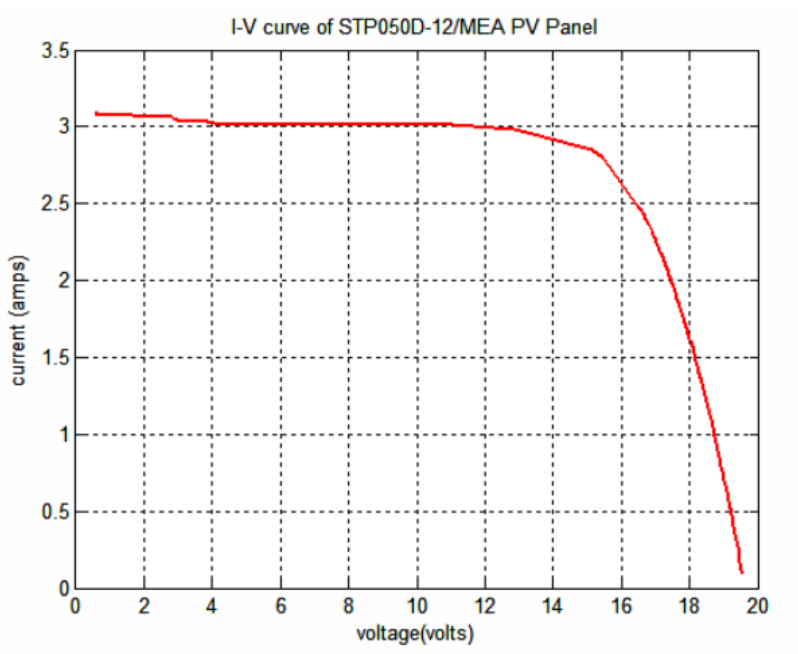

Figure 2.10: Experimental I-V curve obtained on a sunny day [13]

The experiment has then been conducted in a cloudy day and the following results were obtained

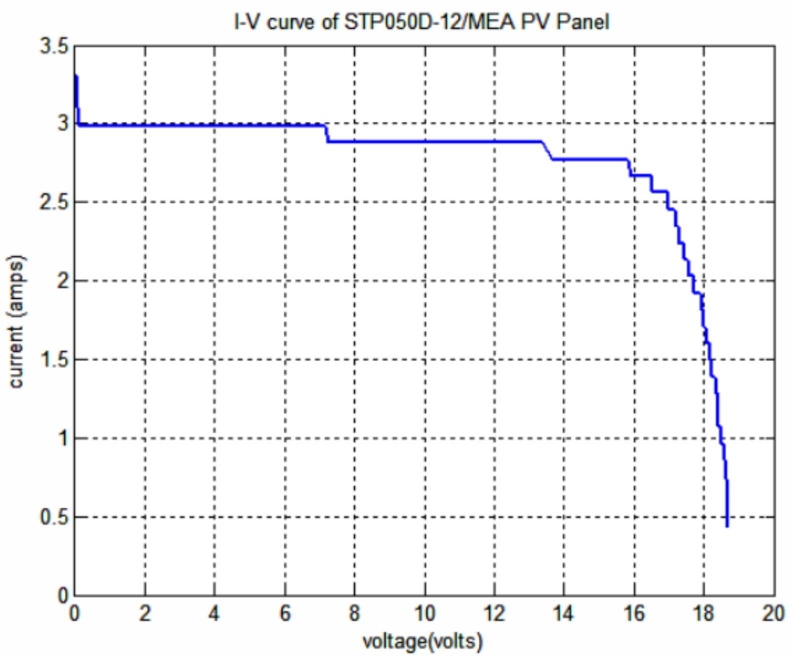

Figure 2.11: Experimental I-V curve obtained on a cloudy day [13]

Comparing the two curves obtained in different conditions and locations gives us a clear idea about the effect of shading on the I-V curve that will be used later to extract the parameters of the PV module. The comparison can be seen in the figure 2.12.

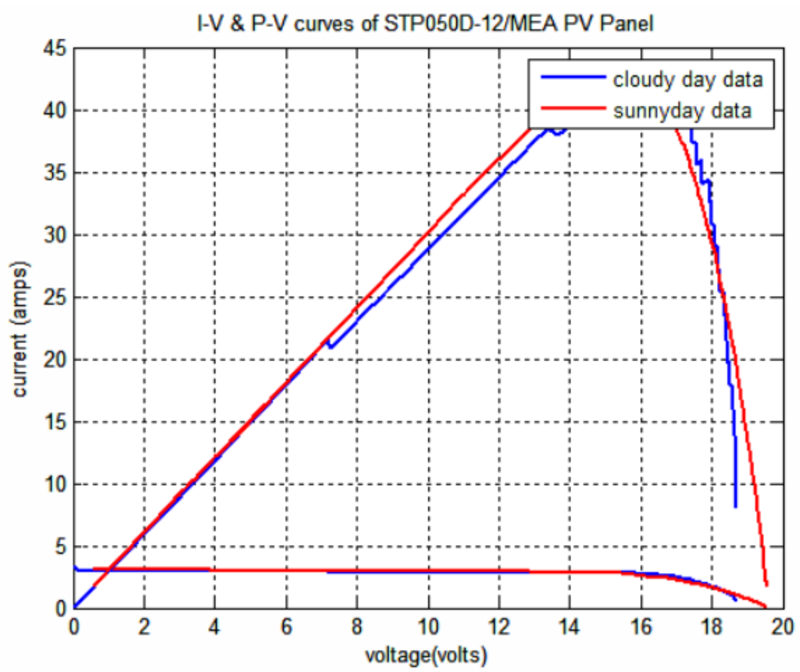

Figure 2.12: comparison between the curves obtained in sunny and cloudy days [13]

2.5 Conclusion

In this chapter, we were able to see the modelling of a PV panel as well as the circuit that allows us to draw the I-V curve using the needed software. We were also able to notice the difference between the ideal curve obtained under optimal conditions, and the curve obtained in virtual shading effect by changing the irradiance input. The obtained results confirmed what has been said in the first chapter on the negative impact of shading on a PV system.

In the second part of the chapter a detailed explanation of the steps followed and material used to obtain the I-V curve has been given. The data obtained from this experiment are to be used in order to identify the parameters of the PV panel in the next chapter.

Chapter Three

PV Parameters Identification

3.1 Introduction

The identification of five parameters of a single-diode model are of prime importance to analyze the behavior of a photovoltaic systems and essential for assessing their efficiency and performance under various operating conditions.

The determination of these parameters is not a trivial task as they are not found on the module data sheet. Generally, two types of algorithms are used to define these parameters, the first are called “local algorithms” which rely on the module’s data sheet, and the second are “the global algorithms” which extract these parameters using the module’s I-V data.

In this chapter, we will use five global algorithms and one local algorithm for the sake of comparison. While the local algorithm solves a system of non-linear equations, all of our five global algorithms are metaheuristic population-based algorithms and will be used to extract parameters from ten PV modules.

3.2 Local Algorithm

As mentioned in the introduction, the local algorithm solves a system of non-linear equations. while there are different methods to extract this system of equations, we have chosen to use the analytical-numerical approach for the five parameters R_s, R_p, A, I_{ph} and I_s determination [16].

This method mainly uses the “fsolve” function on MATLAB to solve the three equations system derived from the approach stated above [16]. The three equations are as following:

$$\frac{I_m}{V_m} - \frac{1}{AN_sV_t}\left(1 - \frac{R_s I_m}{Vm}\right)\left(\frac{-V_{oc}+(R_s+R_p)I_{sc}}{Rp}\right)e^{\frac{V_m - V_{oc} + R_s I_m}{AN_sV_t}} - \frac{1}{Rp}\left(1 - \frac{R_s I_m}{Vm}\right) = 0 \qquad (3.1)$$

$$-I_m\left(1 + \frac{R_s}{R_p}\right) + \left(\frac{-V_{oc}+(R_s+R_p)I_{sc}}{R_p}\right)\left(1 - e^{\frac{-V_{oc}+(R_s+R_p)I_{sc}}{AN_sV_t}}\right) + \frac{V_{oc}-V_m}{R_p} = 0 \qquad (3.2)$$

$$-\frac{R_s}{R_p} + \frac{R_p - R_s}{AN_sV_t}\left(\frac{-V_{oc}+(R_s+R_p)I_{sc}}{R_p}\right)e^{\frac{R_sI_{sc}V_{oc}}{AN_sV_t}} = 0 \qquad (3.3)$$

The algorithm first finds the values of R_s, R_p and A using “fsolve”. The values found will be used to calculate I_{ph} and I_s. Using current divider and ignoring the small value of I_s we can write [16]:

$$I_{ph} = \frac{R_p - R_s}{R_p} I_{sc} \tag{3.4}$$

We can write equation (1.1) as follow to find I_s:

$$I_s = \left(\frac{-V_{oc} + (R_s + R_p)\, I_{sc}}{R_p}\right) e^{-\frac{V_{oc}}{A\, N_s\, V_t}} \tag{3.5}$$

Figure 3.1 shows the local algorithm flowchart.

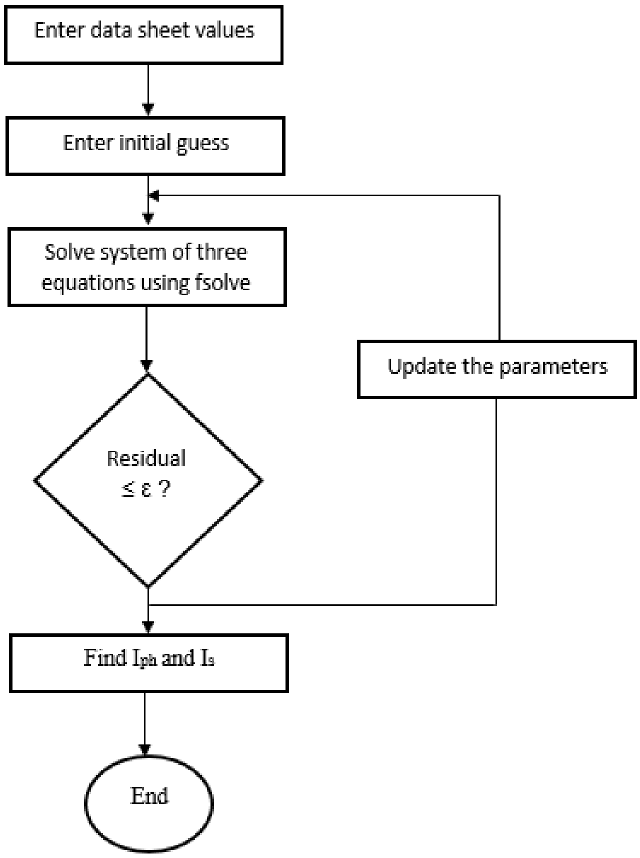

Figure 3.1: Flowchart for local search parameters identification.

3.2.1 Parameters Identification Using Local Algorithm

In this section, the local algorithm will be used to extract the parameters for ten PV modules. The table below shows the modules used and their data sheet values as provided by the manufacturer:

Table 3.1: Data Sheet values of ten PV modules as provided by manufacturer.

PV Module	Voc(V)	Isc(A)	Vm(V)	Im(A)	Ns	Pm(W)	G(W/m²)	T(C°)
Canadian Solar CS6P-265	37.7	9.23	30.6	8.66	60	265	1000	25
LDK-175D-24	44.7	5.43	35.9	4.87	72	175	1000	25
Perllight PLM-250P-60	37.58	8.49	31.73	7.88	60	250	1000	25
Kyocera KD135SX-UPU	22.1	8.37	17.7	7.63	36	135	1000	25
QSmart 95	71.5	1.653	56.6	1.357	119	76.80	950	56
SHARP NU-180E1	30.2	8.54	24	7.71	48	180	1000	48
Solarex MSX-60	21.1	3.8	17.1	3.5	36	60	980	31
SUNPOWER E19/240	48.6	6.30	40.5	5.93	72	240	1000	25
SUNTECH STP050D	19.56	3.063	15.4080	2.8110	33	43.312	950	30
Yingli 185 P-23b	29.5	8.45	23.5	7.87	48	185	1000	25

In order to check the accuracy of our algorithms, we have used the normalized-root-mean-square error (NRMSE) defined as follow:

$$nRMSE\ (\%) = \frac{\sqrt{1/_N\ \sum_{i=1}^{N}(I - Iexp)^2}}{\sqrt{1/_N\ \sum_{i=1}^{N} Iexp^2}} \times 100 \tag{3.6}$$

Where N is the number of measurements, I is the calculated value and I_{exp} is the experimental data.

The table (3.2) shows the identified parameters and the error with the ten PV modules obtained by the local algorithm.

Table 3.2: Identified parameters using local algorithm.

PV Module	Rs(Ω)	R_p(Ω)	A	I_{ph}(A)	I_0(A)	**Error (%)**
Canadian Solar CS6P-265	0.2187	3.0948e+3	1.2063	9.2307	1.4329e-08	**7.3211**
LDK-175D-24	0.1589	284.96	1.7381	5.433	4.8119e-06	**9.7726**
Perllight PLM-250P-60	0.0055	314.67	1.3459	8.4901	1.1308e-07	**1.6049**
Kyocera KD135SX-UPU	0.0895	188.9308	1.5786	8.3740	2.1911e-06	**4.0500**
QSmart 95	0.1998	335.0044	1.9559	1.6540	1.0167e-05	**6.2847**
SHARP NU-180E1	0.1223	175.4163	1.7122	8.5460	5.1178e-06	**8.9383**
Solarex MSX-60	0.1695	637.5705	1.4043	3.8010	3.2976e-07	**1.9122**
SUNPOWER E19/240	0.2098	5319.5	1.2990	6.3002	1.0273e-08	**6.5674**
SUNTECH STP050D	0.3830	833.6096	1.4141	3.0644	2.4830e-07	**5.8837**
Yingli 185 P-23b	0.2268	1.4291e+03	1.2640	8.4513	5.0594e-08	**8.4128**

The figure 3.2 shows the extent of match between the I-V curve extracted by the algorithm (blue curve) and the experimental I-V curve (red circles) for Kyocera KD135SX-UPU (error 4.05%)

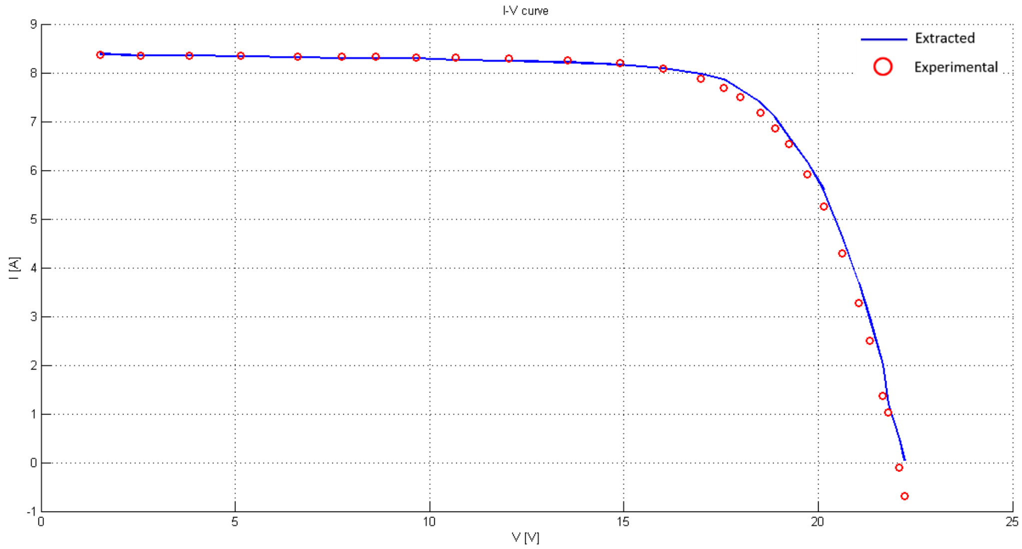

Figure 3.2: Theoretical and experimental I-V curves for Kyocera KD135SX-UPU (error 4.05%)

From the results, it is observed that the local algorithm provides accurate results with some PV modules (less than 2% with Perllight PLM-250P-60 and Solarex MSX-60) but less accurate with some others (9.77% with LDK-175D-24). The average error of the results extracted by the local algorithm is 6.07 % in an average time of 0.45 second.

3.3 Global Algorithms

Global optimization is a branch of applied mathematics and numerical analysis that deals with the global optimization of a function or a set of functions according to some criteria. Typically, a set of bound and more general constraints is also present, and the decision variables are optimized considering also the constraints. It is distinguished from regular optimization by its focus on finding the maximum or minimum over all input values, as opposed to finding local minima or maxima [17].

As we have observed before, the local algorithm is limited in terms of accuracy of results, with an error up to 9.77% (LDK-175D-24) and exceeding 5% with all PV modules not working under STC. The inability of local algorithm to estimate parameters with a high accuracy is what made scientists and researchers interested more in global algorithms.

In this section, we will use five global algorithms in order to extract our parameters: Firefly Algorithm, Differential Evolution, Particle Swarm Optimization, Exchange Market Algorithm and the Bees Algorithm; Our objective function to be minimized by the algorithms is the Normalized Root Mean Square Error function. It will be used with all our global algorithms. We will also use one equation (3.7) with all algorithms in order to derive our parameters.

$$I = N_p \times I_{ph} - N_p \times I_s \left(e^{\frac{\frac{V}{N_S} + \frac{IR_S}{N_p}}{AV_t}} - 1 \right) - \frac{\frac{N_p V}{N_S} + R_S I}{R_p} \tag{3.7}$$

3.3.1 Parameters Identification Using the Firefly Algorithm

The firefly algorithm is a metaheuristic developed by Xin-She Yang in late 2007. It is inspired from the flashing patterns and behavior of fireflies [18]. For our search, we have used a standard Firefly Algorithm which uses three idealized rules [18]:

1- All fireflies are attracted to each other.
2- Attractiveness is proportional to the firefly's brightness. The less bright firefly will move toward the brighter.
3- The attractiveness of a firefly is determined by the objective function. In our case, as we are trying to minimize the objective function, the brightness is disproportional to the value of the objective function, the firefly with less error is the brighter.

The initial position of fireflies is randomly generated. Each firefly represents a candidate solution with a certain degree of error.

The attractiveness of the firefly is determined by its brightness (3.8) which is proportional to the light intensity (3.9). The brightness is the main factor that updates the position of fireflies and make them move towards the brightest as expressed in the position function (3.10) [18].

$$\beta(r) = \beta_0 e^{-\gamma r^2} \tag{3.8}$$

$$I = I_0 e^{-\gamma r^2} \tag{3.9}$$

$$x_i^{t+1} = x_i^t + \beta_0 e^{-\gamma r_{ij}^2} \left(x_j^t - x_i^t \right) + \alpha \epsilon_i^t \tag{3.10}$$

Where:

r is the distance of light source.

r_{ij} is the distance between firefly i and firefly j.

β_0 is the attractiveness at r = 0.

I_0 is the original light intensity at zero distance r = 0.

γ is the light absorption coefficient.

α is the randomization parameter.

ϵ is a vector of random numbers drawn from a Gaussian distribution or uniform distribution. [18]

Based on these idealized rules and the equations, the pseudo code of the firefly algorithm can be written as follow [18]:

Firefly Algorithm
Objective function *: N*RMSE function
Generate an initial population of *n* fireflies ***xi*** (*i* = 1, 2, ..., *n*).
Light intensity *Ii* at ***xi*** is determined by *f*(***xi***).
Define light absorption coefficient *γ*.
while (*t* <MaxGeneration),
for *i* = 1 : *n* (all *n* fireflies)
for *j* = 1 : *n* (all *n* fireflies) (inner loop)
if (*Ii* < *Ij*)
Move firefly *i* towards *j*.
end if
Vary attractiveness with distance *r* via exp[−*γr*2].
Evaluate new solutions and update light intensity.
end for j
end for i
Rank the fireflies and find the current global best ***g*** *∗*.
end while
Postprocess results and visualization

Figure 3.3: Pseudo code of the Firefly Algorithm.

The table (3.3) shows the identified parameters and the error with the ten PV modules after executing the firefly algorithm.

Table 3.3: Identified parameters using the Firefly Algorithm.

PV Module	Rs(Ω)	Rp(Ω)	A	Iph(A)	I0(A)	Error (%)
Canadian Solar CS6P-265	0.0635	803.03	1.4499	9.4605	4.9985e-07	**2.5701**
LDK-175D-24	0.1194	451.61	1.8345	5.2038	1.0912e-05	**4.3328**
Perllight PLM-250P-60	0.0635	491.58	1.2828	8.5084	4.585e-08	**0.9681**
Kyocera KD135SX-UPU	0.0858	698.06	1.5006	8.2629	9.4024e-07	**1.4831**
QSmart 95	0.0709	559.35	1.9924	1.6457	3.9091e-05	**5.3201**
SHARP NU-180E1	0.1191	492.8	1.9199	8.3519	2.6148e-05	**1.6993**
Solarex MSX-60	0.0676	319.55	1.7172	3.8719	6.4579e-06	**1.5947**
SUNPOWER E19/240	0.0522	396.58	1.8329	6.2115	3.3764e-06	**2.2218**
SUNTECH STP050D	0.1171	743.15	1.5853	3.0537	5.9668e-06	**5.3249**
Yingli 185 P-23b	0.0597	413.27	1.7224	8.1917	7.7206e-06	**3.2315**

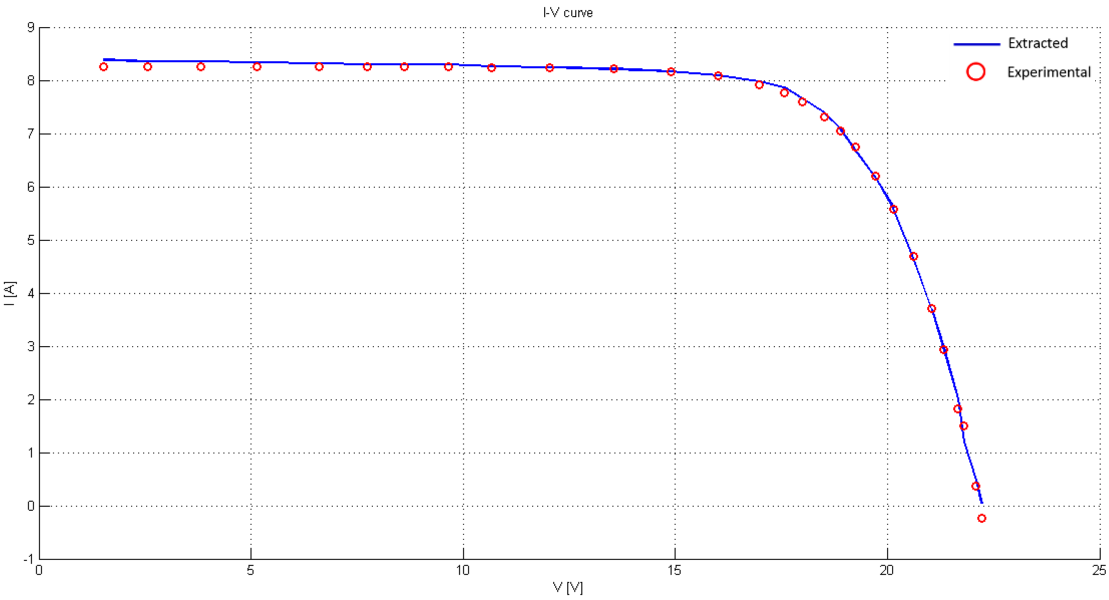

Figure 3.4: Theoretical and experimental I-V curves for Kyocera KD135SX-UPU (error 1.48%)

The Firefly Algorithm converges to highly accurate results after an average time of execution of 20.09 seconds. These results are more precise than the local algorithm as the NRMS error does not exceed 5.33% and the average error is 2.87%.

3.3.2 Parameters Identification Using the Differential Evolution

Differential Evolution or DE was developed by R. Storn and K. Price in 1996. Due to their similar search pattern, DE is considered as a further development to the Genetic Algorithm.

It is a vector-based metaheuristic algorithm. In our case, the five parameters vector are considered as chromosomes. The Differential evolution consists mainly of three steps [18]:

1. Mutation: a donor-vector v_i^{t+1} is generated by: [18]

$$v_i^{t+1} = x_p^t + F(x_q^t - x_r^t) \tag{3.11}$$

Where x_p^t, x_q^t *and* x_r^t are randomly generated vectors.

2. Crossover: random exchange of vector components is done with the donor vector following the scheme: [18]

$$u_{j,i}^{t+1} = \begin{cases} v_{i,j} & if\ r_i \leq C_r, \\ x_{j,i}^t & Otherwise \end{cases} \quad j = 1,2,\dots,5. \tag{3.12}$$

Where C_r is the crossover coefficient ∈ [0, 1] and r random number between 0 and 1.

3. Selection: vector with the most accurate parameters (minimum NRMS error) are selected as following: [19]

$$x_i^{t+1} = \begin{cases} u_i^{t+1} & if\ f(u_i^{t+1}) \leq f(x_i^t), \\ x_i^t & Otherwise \end{cases} \tag{3.13}$$

The pseudo code of the Differential Evolution is as shown below:

Differential Evolution
Initialize the population ***x*** with randomly generated solutions
Set the weight $F \in [0, 2]$ and crossover probability $Cr \in [0, 1]$
while (stopping criterion)
for $i = 1$ to n,
For each ***xi***, randomly choose 3 distinct vectors ***xp***, ***xr*** and ***xr***
Generate a new vector ***v*** by DE scheme (3.11).
Generate a random index J
$r \in \{1, 2, ..., d\}$ by permutation
Generate a randomly distributed number $ri \in [0, 1]$
for $j = 1$ to d,
For each parameter ***v****j*,*i* (*j*th component of ***v****i*), update $u_{j,i}^{t+1}$ using (3.12).

end
Select and update the solution by (3.13)
end
end
Post-process and output the best solution found.

Figure 3.5: Pseudo code of the Differential Evolution.

The table (3.4) shows the identified parameters and the error with the ten PV modules after executing the Differential Evolution.

Table 3.4: Identified parameters using the Differential Evolution.

PV Module	Rs(Ω)	Rp(Ω)	A	Iph(A)	I0(A)	**Error (%)**
Canadian Solar CS6P-265	0.0283	986.86	1.5285	9.3419	1.1783e-06	**2.6337**
LDK-175D-24	0.3637	223.46	1.5111	5.2101	6.2257e-07	**4.1121**
Perllight PLM-250P-60	0.0057	559.65	1.4681	8.5072	5.121e-07	**1.078**
Kyocera KD135SX-UPU	0.1027	846.85	1.4498	8.1919	5.1514e-07	**1.9258**
QSmart 95	4.2322	886.65	1.4634	1.6647	8.3611e-07	**1.0869**
SHARP NU-180E1	0.14816	955.53	1.6468	8.2253	3.2014e-06	**1.6067**
Solarex MSX-60	0.20974	681.11	1.3894	3.8302	2.7914e-07	**0.5210**
SUNPOWER E19/240	0.18051	849.94	1.7048	6.1078	1.1146e-06	**1.9502**
SUNTECH STP050D	0.4357	963.9	1.3658	3.0527	6.5899e-07	**2.824**
Yingli 185 P-23b	0.060589	127.4	1.6682	8.2558	4.7134e-06	**3.2799**

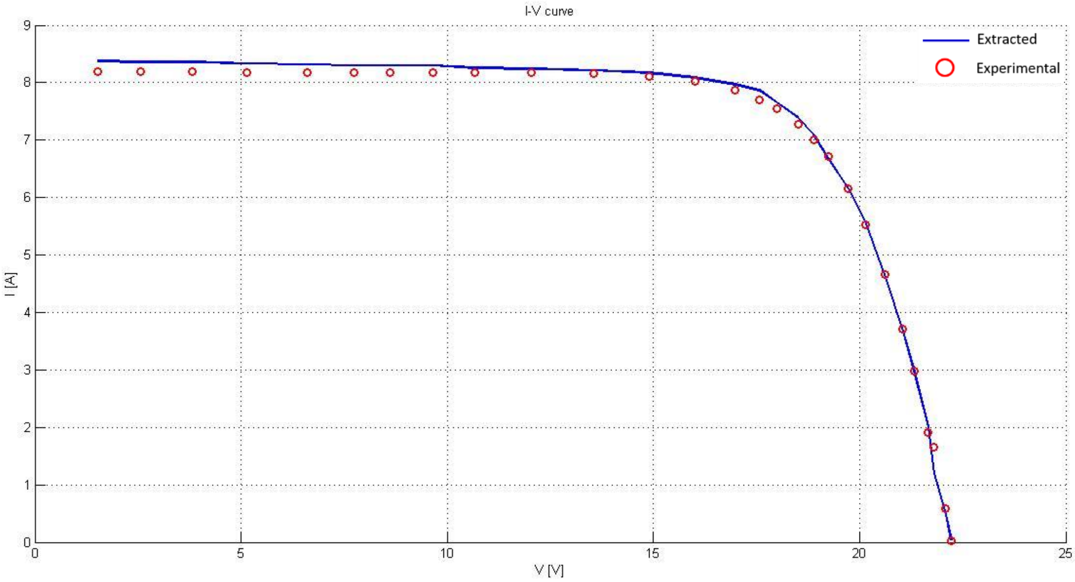

Figure 3.6: Theoretical and experimental I-V curves for Kyocera KD135SX-UPU (error 1.93%)

Results are extracted by the Differential evolution in an average time of 3.07 seconds with an error not exceeding 4.12% and an average of only 2.1%.

3.3.3 Parameters Identification Using the Particle Swarm Optimization

Particle swarm optimization (PSO) was developed by Kennedy and Eberhart in 1995 based on swarm behavior in nature, such as fish and bird schooling. Since then, PSO has generated much wider interests and forms an exciting, ever-expanding research subject, called swarm intelligence. PSO has been applied to almost every area in optimization, computational intelligence, and design applications. [18].

The PSO algorithm adjusts the trajectory of particles so that it is attracted toward the position of the current global best. In our case, the global best is the least NRMS error and the position corresponding to it is the solution to our search of the five parameters. The movement of the particle is determined by its velocity (3.14) which updates the position of the particle (3.15).

$$v_i\ (k+1) = wv_i\ (k) + c_1 r_1\ [L_i(k) - x_i\ (k)] + c_2\ r_2\ [G(k) - x_i\ (k)] \qquad (3.14)$$

$$x_i\ (k+1) = x_i\ (k) + v_i\ (k+1) \qquad (3.15)$$

Where:

xi is the position of the i^{th} particle in the search space.

vi is the velocity of the i^{th} particle.

c_1 is cognitive acceleration constant.

c_2 is social acceleration constant.

L_i is particle's best known position.

w being the particle inertia.

G is the best-known position found by all particles.

r_1 , r_2 are random number between 0 and 1. [18]

Based on this information, the pseudo code of the PSO algorithm can be written as follow [18]:

Particle Swarm Optimization
Objective function *: NRMSE funciton*
Initialize locations ***xi*** and velocity ***vi*** of *n* particles.
Find $\boldsymbol{g}*$ from min*{f*(***x***1),...,*f*(***x****n*)*}* (at *t* = 0)
while (criterion)
for loop over all *n* particles and all *d* dimensions
Generate new velocity ***vt*** *i*+1 using equation (3.14)
Calculate new locations ***x****t*+1 using equation (3.15)
Evaluate objective functions at new locations ***xt*** *i*+1
Find the current best for each particle $\boldsymbol{x}*\,i$
end for
Find the current global best $\boldsymbol{g}*$
Update *t* = *t* + 1 (pseudo time or iteration counter)
end while
Output the final results $\boldsymbol{x}*\,i$ and $\boldsymbol{g}*$

Figure 3.7: Pseudo code of the PSO.

The table (3.5) shows the identified parameters and the error with the ten PV modules after executing the PSO algorithm.

Table 3.5: Identified parameters using the PSO Algorithm.

PV Module	Rs(Ω)	R_p(Ω)	A	I_{ph}(A)	I_0(A)	**Error (%)**
Canadian Solar CS6P-265	0.0553	1498.9	1.4651	9.4145	5.935e-07	**2.5185**
LDK-175D-24	0.3656	1499.8	1.6849	5.3358	3.3727e-06	**2.6736**
Perllight PLM-250P-60	0.0413	337.86	1.3007	8.5123	6.0777e-08	**0.6979**
Kyocera KD135SX-UPU	0.0979	176.9	1.4751	8.3631	7.0142e-07	**1.2536**
QSmart 95	4.542	1262.8	1.3877	1.6546	3.8117e-07	**0.9552**
SHARP NU-180E1	0.1537	122.52	1.6024	8.4192	2.151e-06	**0.8264**
Solarex MSX-60	0.17	899.99	1.4780	3.8329	7.5441e-07	**0.6930**
SUNPOWER E19/240	0.2028	1500	1.7061	6.2	1.1497e-06	**1.2563**
SUNTECH STP050D	0.4051	879.99	1.4262	3.0556	1.2624e-06	**2.8427**
Yingli 185 P-23b	0.025	49.626	1.6791	8.427	5.2409-06	**2.8481**

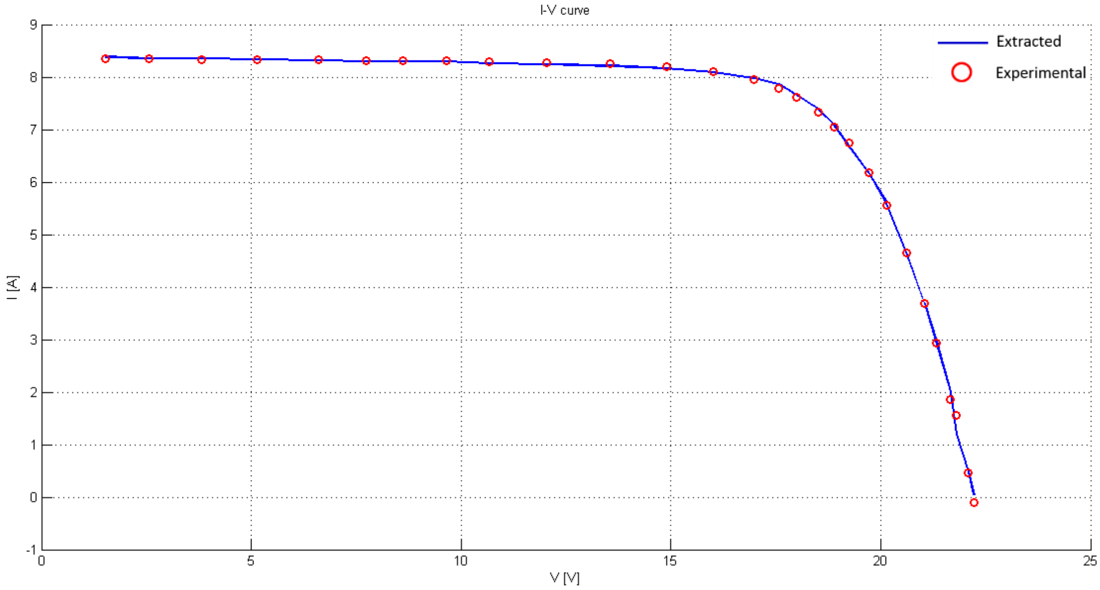

Figure 3.8: Theoretical and experimental I-V curves for Kyocera KD135SX-UPU (error 1.25%)

The Particle Swarm Optimization Algorithm converges after only 0.73 second average execution time and estimates with high accuracy our parameters. The parameters extracted using this algorithm exhibit an NRMS error of less than 2.85% and an average error is 1.66%.

3.3.4 Parameters Identification Using the Exchange Market Algorithm

The Exchange Market Algorithm was developed in 2014 by Naser Ghorbani and Ebrahim Babae. The EM algorithm is inspired by shares traded on the stock market in which the shareholders buy and sell several types of shares in the virtual stock market under different market conditions. It is assumed that the shareholders compete to introduce themselves as the most successful dealers in the ranking list by a continuous learning from the high ranked shareholders. Shareholders will operate under two marker conditions: balanced condition and oscillated condition, and behave differently according to the market they are established in. In our case, the best shareholders are those with the less NRMS error (or the best shares) [19].

First, the shareholders take a number of any type of shares (in our case the five parameters) randomly. All shares are solutions with a certain degree of error. After that, shareholders' costs are evaluated and ranked into three groups: high, mean, and low according to their costs.

Under balanced market condition, group 2 and group 3 members adjust their shares according to (3.16) and (3.17) respectively, while group 1 shareholders remain unchanged. [19]

$$pop_j^{group(2)} = r \times pop_{1,i}^{group(1)} + (1-r) \times pop_{2,i}^{group(1)} \quad , \quad i = 1,2,3, \dots n_i \; and \; j = 1,2,3, \dots n_j \qquad (3.16)$$

Where:

$n_i$is the n^{th} person of the first group.

n_j is the n^{th} person of the second group.

r is a random number in interval [0, 1].

$pop_{1,i}^{group(1)}$and $pop_{2,i}^{group(1)}$are the i^{th} person of the first group.

$pop_j^{group(2)}$ is the j^{th} person of the second group.

$$pop_k^{group(3),new} = pop_k^{group(3)} + 0.8 \times Sk \qquad (3.17)$$

Such that: [19]

$$S_k = 2 \times r_1 \times (pop_{1,i}^{group(1)} - pop_k^{group(3)}) + 2 \times r_2 \times (pop_{1,2}^{group(1)} - pop_k^{group(3)})$$
(3.18)

Where:

r_1 and r_2 are random numbers in interval [0, 1].

$pop_k^{group(3)}$is the k^{th} member of the third group.

S_k is the share variations of the k^{th} member of the third group.

After group 2 and 3 change their shares, they are evaluated and ranked. The aim of this step is to find the best shareholders in the balanced market. [19]

Under oscillation market condition, group 2 and group 3 members adjust their shares according to (3.19) and (3.24) respectively, while group 1 shareholders remain unchanged [19].

$$\Delta n_{t1} = n_{t1} - \delta + (2 * r * \mu * \eta_1) \tag{3.19}$$

Such that:

$$\mu = \frac{t_{pop}}{n_{pop}} \tag{3.20}$$

$$n_{t1} = \sum_{y=1}^{n} S_{ty}\,, \quad y = 1,2,3, \dots, n \tag{3.21}$$

$$\eta_1 = n_{t1} \times g_1 \tag{3.22}$$

$$g_1^k = g_{1,max} - \frac{g_{1,max} - g_{1,min}}{iter_{max}} \times k \tag{3.23}$$

Where:

Δn_{t1} is the amount of shares should be added randomly to some shares.

n_{t1} is total shares of the t^{th} member before applying the share changes.

δ is the information of exchange market.

r is a random number in interval [0, 1].

η_1 is risk level related to each member of the second group.

μ is a constant coefficient for each member.

t_{pop} is the number of the t^{th} member in exchange market.

n_{pop} is the number of the last member in exchange market.

S_{ty} is the shares of the t^{th} member

g_1 is the common market risk amount which decreases as iteration number increases.

$iter_{max}$ is the last iteration number.

k is the number of program iteration.

$g_{1,max}$ and $g_{1,min}$ indicate the maximum and minimum values of risk in market, respectively.

$$\Delta n_{t3} = (4 * r_s * \mu * \eta_2) \qquad (3.24)\ [19]$$

Such that: [19]

$$r_s = 0.5 - rand \qquad (3.25)$$

$$\eta_2 = n_{t1} \times g_2 \qquad (3.26)$$

Where:

Δn_{t3} is the share amount that should be added randomly to the shares of each member.

g_2 is the variable market risk amount which decreases as iteration number increases.

r_s is a random number in interval [-0.5, 0.5].

η_2 is risk level related to each member of the third group.

μ is a constant coefficient for each member.

After group 2 and 3 change their shares, the termination criteria is checked, if satisfied the program ends up and displays results. If not, shareholders are evaluated and ranked to operate under balanced market condition and repeats the loop [19]. Accordingly, the general principle of the Exchange Market Algorithm can be described as following [19]:

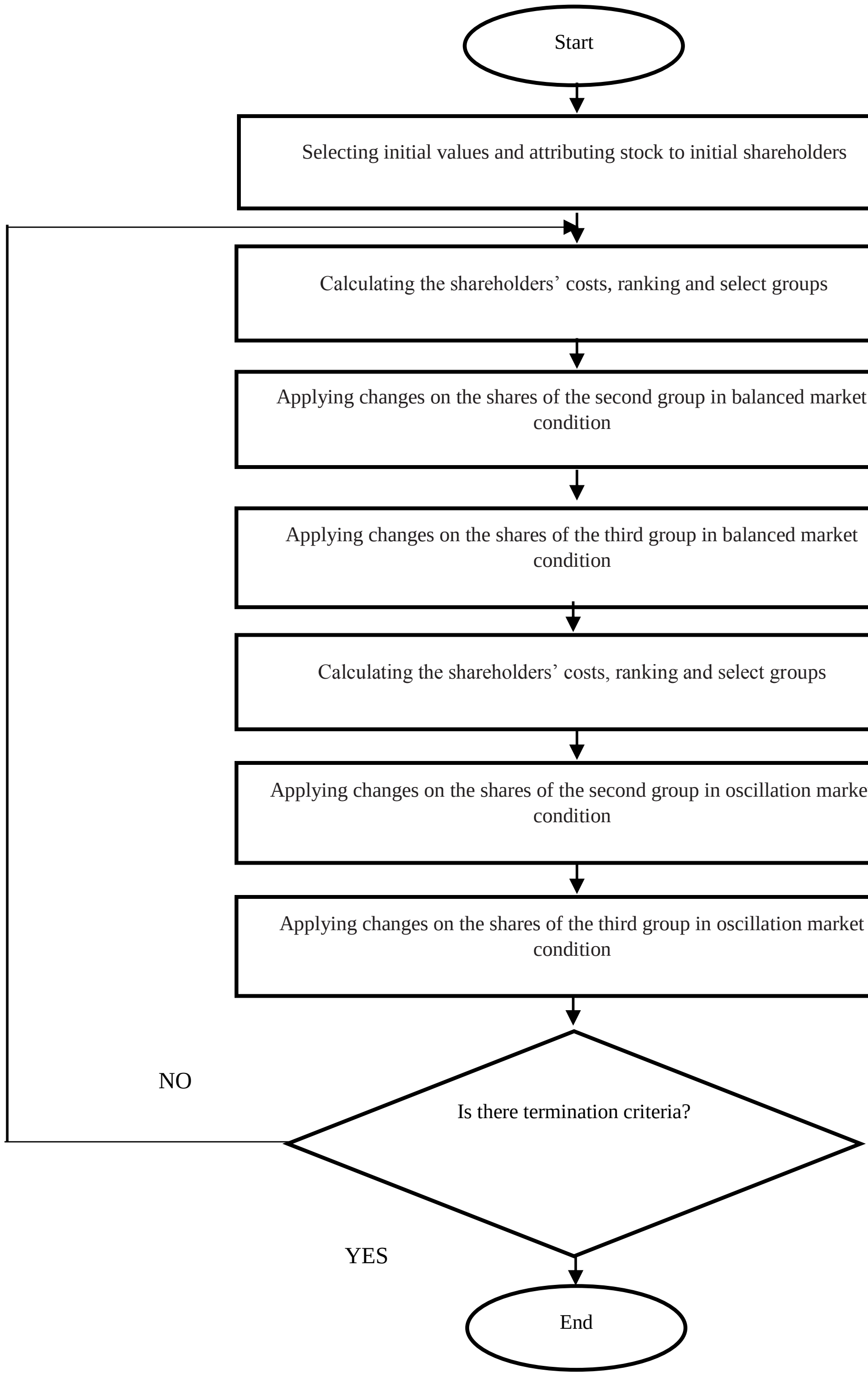

Figure 3.9: Flowchart of the Exchange Market Algorithm.

After the EMA is adapted to our search, the following results are obtained:

Table 3.6: Identified parameters using the Exchange Market Algorithm.

PV Module	Rs(Ω)	Rp(Ω)	A	Iph(A)	I0(A)	**Error (%)**
Canadian Solar CS6P-265	0.0329	1500	1.5373	9.4276	1.3028e-06	**2.4983**
LDK-175D-24	0.4366	1499.9	1.5510	5.3241	9.7764e-07	**2.4354**
Perllight PLM-250P-60	0.052	265.89	1.2570	8.5197	3.1596e-08	**0.7029**
Kyocera KD135SX-UPU	0.0972	205.97	1.4818	8.3573	7.5565e-07	**1.3558**
QSmart 95	4.3683	1272.28	1.4466	1.6556	7.1018-07	**0.9793**
SHARP NU-180E1	0.1326	669.63	1.7289	8.3445	6.6176e-06	**0.8032**
Solarex MSX-60	0.2142	1500	1.3734	3.8133	2.3112e-07	**0.3577**
SUNPOWER E19/240	0.2163	1500	1.6807	6.1957	9.0593e-07	**1.2544**
SUNTECH STP050D	0.4684	868.12	1.3017	3.0502	3.0769e-07	**2.83**
Yingli 185 P-23b	0.01	59.958	1.7698	8.3989	1.099-05	**2.6337**

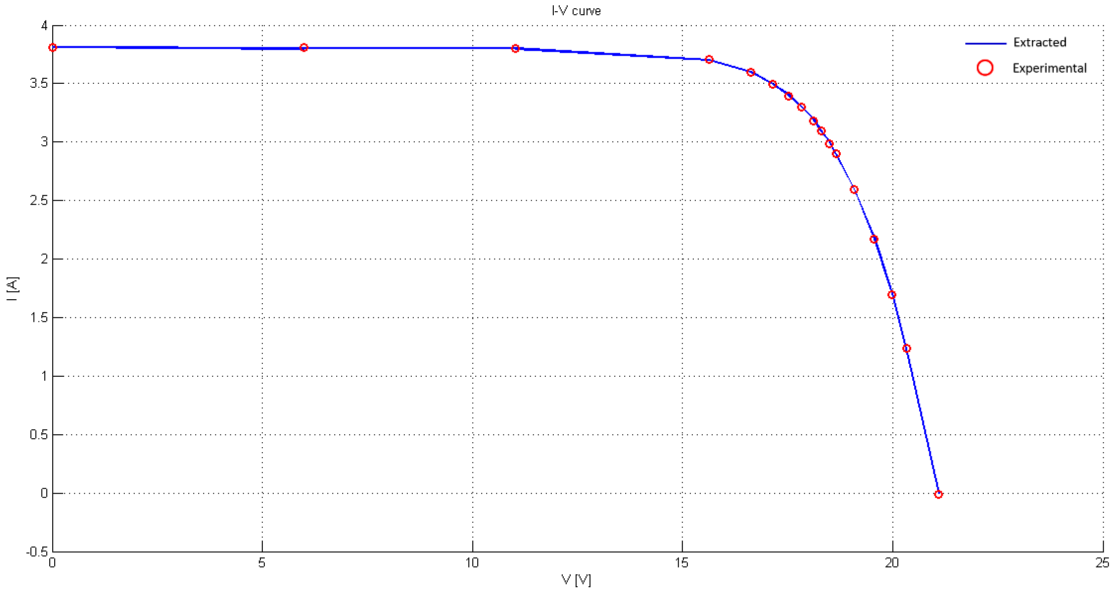

Figure 3.10: Theoretical and experimental I-V curves for Solarex MSX-60 (error 0.36%).

As the results illustrate, the Exchange Market Algorithm converges to very accurate results. The. the NRMS error does not exceed 2.64% and the average error is 1.59% and average execution time is 3.26 seconds.

3.3.5 Parameters Identification Using the Bees Algorithm

The Bees Algorithm or BA is a population based algorithm developed in 2005 and inspired from the foraging behavior of bees. The BA mimics the foraging strategy of honey bees to look for the best solution to an optimization problem. Each time an artificial bee visits a flower in its search space (in our case a vector of the five parameters), it evaluates its profitability (NRMS error). The foraging process is achieved by scout bees which represent a percentage of the bees colony. When scouting bees return to the hive, the perform “the waggle dance” to communicate the quality and the place of the best patches they have found. Onlooker bees present in the hive evaluate dances and send more bees to the most profitable patch to perform further exploration (less NRMS error in our case). If it is the case, more scout bees are recruited to that source until no better flower is found (minimum NRMS Error and most accurate parameters). If not, employed bees will be directed to a richer patch accidently discovered by remaining scouts and process repeats [20].

Based on this description, the pseudo code of the Bees algorithm can be written as below [21]:

The Bees Algorithm
Generate the initial population xi (i = 1, 2, . . . , SN)
Evaluate fitness of initial population.
While (selection criterion)
For each employed bee {
Produce new solution Vi by using (3.27)
Calculate its fitness value fit(Vi)
Apply greedy selection process}
Calculate the probability values Pi for the solution (xi) by (3.28)
For each onlooker bee {
Select a solution xi depending on Pi
Produce new solution Vi
Calculate its fitness value fit(Vi)
Apply greedy selection process}
If there is an abandoned solution for the scout,
Then replace it with a new solution which will be randomly produced.
Memorize the best solution so far
End
Display best solution
End

Figure 3.11: Pseudo code of the Bees Algorithm.

Accordingly, three main search phases define the Bees Algorithm [21]:

1. Search phase of Employed Bees: neighbor food source is created from initial food source by [21]:

$$v_i^j = x_i^j + \varphi_i^j (x_i^j - x_k^j) \tag{3.27}$$

Where $j \in \{1, 2, . . . \ d\}$ and $k \in \{1, 2, . . . , SN\}$ are randomly chosen indexes. Although k is determined randomly, it has to be different from i. φ_i^j is a random number in the range $[-1, 1]$ [21].

2. Search phase of Onlooker Bees: Onlooker bees select the best patches based on fitness probability selection defined as [21]:

$$P_i = \frac{fit(x_i)}{\sum_{m=1}^{SN} fit(x_m)} \tag{3.28}$$

Where $fit(x_i)$ is the fitness value of solution i.

3. Scout Bee phase: when no better food sources are found by the Onlooker bees, the algorithm checks if the random scout bees have found a richer patch to be explored.

After the BA is adapted to our search, the following results are obtained:

Table 3.7: Identified parameters using the Bees Algorithm.

PV Module	$R_s(\Omega)$	$R_p(\Omega)$	A	I_{ph}(A)	I_0(A)	**Error (%)**
Canadian Solar CS6P-265	0.0469	898.15	1.4911	9.4259	7.9446e-07	**2.5161**
LDK-175D-24	0.5941	668.46	1.274	5.3213	3.2719e-08	**2.0031**
Perllight PLM-250P-60	0.0303	445.82	1.3411	8.5053	1.0764e-07	**0.7262**
Kyocera KD135SX-UPU	0.0948	189.94	1.4933	8.3616	8.5766e-07	**1.2531**
QSmart 95	4.5607	894.53	1.3626	1.6634	2.8579e-07	**0.9892**
SHARP NU-180E1	0.1728	123.58	1.5196	8.4072	9.3956e-07	**0.9245**
Solarex MSX-60	0.2276	961.25	1.3296	3.8113	1.335e-07	**0.3702**
SUNPOWER E19/240	0.2338	963.02	1.6399	6.2018	6.1218e-07	**1.2739**
SUNTECH STP050D	0.4363	925.87	1.3679	3.0526	6.7384e-07	**2.8248**
Yingli 185 P-23b	0.0870	136.08	1.4868	8.219	8.3992e-07	**3.7236**

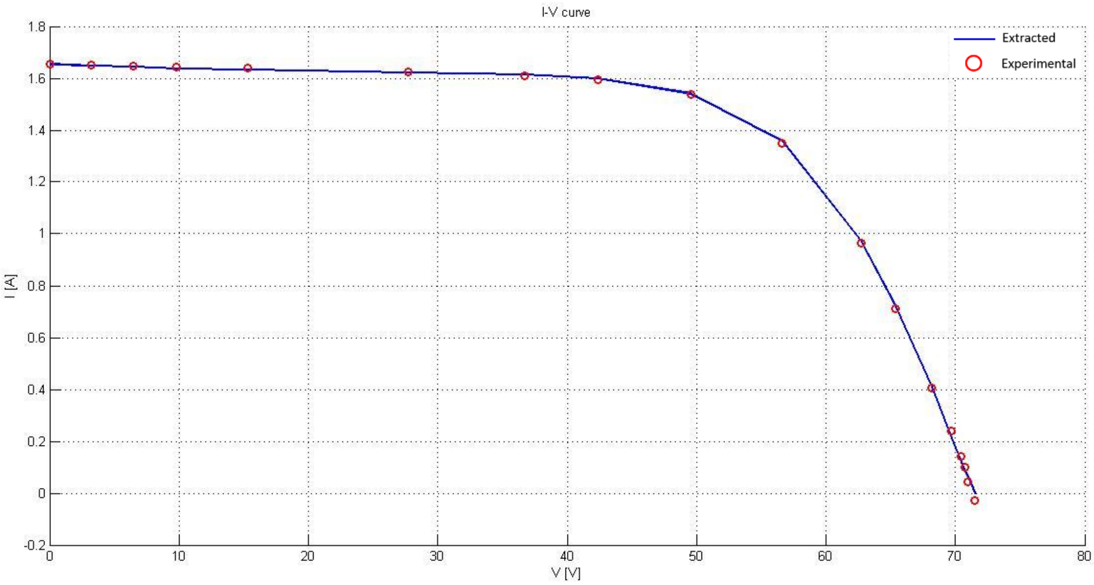

Figure 3.12: Theoretical and experimental I-V curves for QSmart 95 (error 0.9892%).

The Bees Algorithm extract parameters with an average error of 1.66% in an average time of 1.65 seconds.

3.4 Discussion

Table 3.8: Average errors and time execution of the six used algorithms.

Algorithm	Local	FA	DE	PSO	EMA	BA
Average error (%)	6.07%	2.87%	2.1%	1.66%	1.59%	1.66%
Average time of execution (s)	0.45	20.09	3.07	0.73	3.26	1.65

The five global algorithms used to extract I-V curves show satisfactory results not exceeding an average error of 2.87% whereas the local algorithm attained a considerable error of 6.07%.

The local algorithm converged rapidly by simple use of “fsolve” function in MATLAB. The performance of the algorithm varied from a PV module to another. While it did not exceed 2% error with Solarex MSX-60 and Perllight PLM-250P-60, the local algorithm reached high errors of 8.94% with SHARP NU-180E1 and 9.77% with LDK-175D-24. As the “fsolve” function demands an initial guess close to the actual result, the local algorithm is performant only if the initial guess is estimated wisely for each PV module.

Global algorithms demonstrated a higher accuracy than the local. Even if these algorithms are relatively slow comparing the local algorithm (especially the firefly algorithm), parameters are extracted with a high accuracy. Further, the global search algorithms do not require an initial guess to start iteration. They start with random population to converge to an optimal solution.

As illustrated by the results, the Particle Swarm Optimization, Bees Algorithm and Exchange Market Algorithm are the best three algorithms in terms of accuracy (1.59% for EMA, 1.66% for both PSO and BA). In terms of time of execution, the PSO and BA were the fastest among global algorithms (0.73s for PSO and 1.65 for BA). Even though The Exchange Market Algorithm is relatively slow comparing to other global algorithms (time of execution of 3.26 seconds), it performed the best estimation with an average error of 1.59% and extracted 50% of the most accurate parameters as illustrated in figure 3.12.

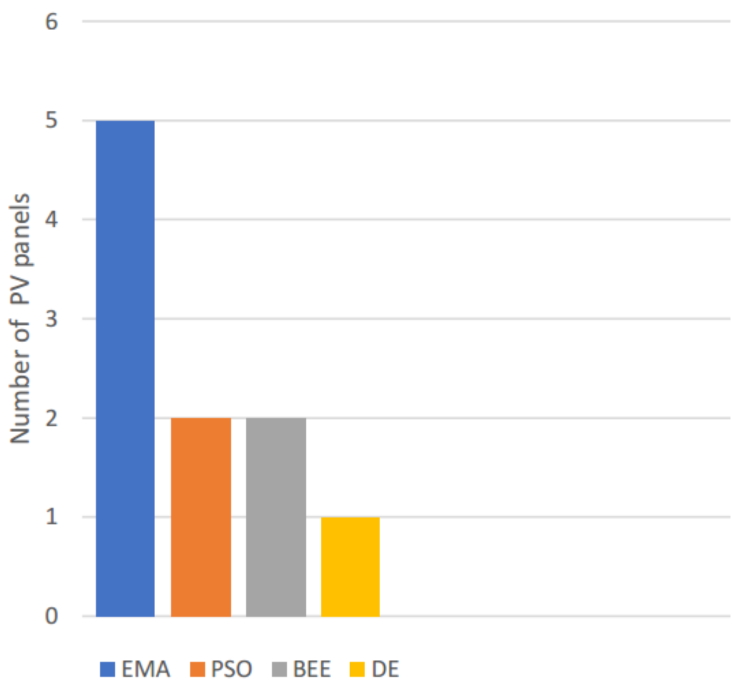

Figure 3.13: Number of best performances for each Algorithm.

3.5 Conclusion

In this chapter, four algorithms were used for the identification of the single-diode PV cell five parameters.

Local algorithm uses few data for a fast extraction. However, the algorithm shows some limitations and requires appropriate initial values to achieve convergence and solve the resulting nonlinear equations. Global algorithms use more data for a relatively slow but highly accurate estimation of parameters without necessity of initial guess. Even though local algorithm provides fast solutions, global algorithms extract a highly accurate estimation of the five parameters. Despite its relatively slow execution, the Exchange Market Algorithm was the most successful in our search.

General Conclusion

General conclusion

Estimating an accurate model parameters is central to the design, manufacturing and evaluation of PV systems as it permits to forecast the behavior of systems under different working conditions.

Obtaining the most accurate five parameters search was the main objective of this project. In this work, we first covered the process of data acquisition by the implemented circuit. in the second part, we identified our single-diode model parameters using the local algorithm that relied on the manufacturer datasheet, and five global algorithms that used the I-V data acquired from the acquisition circuit. Whereas local algorithm displayed a limited performance, global algorithms showed a satisfying estimation as the five parameters were extracted with slight errors. The results have proved that the Particle Swarm Optimization, the Bees Algorithm and the Exchange Market Algorithm are the best algorithms for our search.

Finally, it is to be emphasized that the main objective of this work is achieved as we have employed three global algorithms that extracted PV single-model parameters with high accuracy. For a more accurate identification, we suggest to implement all the three algorithms and output the best result among the three algorithms. The triple-use of these algorithms also allows to operate all the features (fast processing of PSO and BA, high accuracy of EMA), which provides the card user with the possibility to customize his search depending on the operation.

For future work, along with creating a PCB that assembles both the acquisition and the process circuits, a further work on parameters identification is required by the use of more sophisticated search algorithms. The features of the algorithms explored in this work can be combined by developing a hybrid algorithm adapted to the parameters search. Also, performing the process with different accuracy metrics as objective functions contributes to a better assessment of tested algorithms.

References

References

[1] Nef.org.uk. Types of Photovoltaic (PV) Cells - National Energy Foundation. [online] Available at: http://www.nef.org.uk/knowledge-hub/solar-energy/types-of-photovoltaic-pv-cells [May 2017]

[2] Krauter, S C W. (2006). Solar Electric Power Generation – Photovoltaic Energy Systems. Rio de Janeiro: Springer, p21-23.

[3] Association, S. Photovoltaic (Solar Electric). [online] SEIA. Available at: http://www.seia.org/policy/solar-technology/photovoltaic-solar-electric [April 2017]

[4] Fsec.ucf.edu. How PV Cells Work. [online] Available at: http://www.fsec.ucf.edu/en/consumer/solar_electricity/basics/how_pv_cells_work.htm.

[5] Science.nasa.gov. How do Photovoltaics Work? | Science Mission Directorate. [online] Available at: https://science.nasa.gov/science-news/science-at-nasa/2002/solarcells/ [March 2017]

[6] Samlexsolar.com. Power Curves & Characteristics for Solar Cells | Samlex Solar. [online] Available at: http://www.samlexsolar.com/learning-center/solar-panels-characteristics.aspx

[7] Femia, N. and Petrone, G. and Spagnuolo, G. and Vitelli, M. (2013). Power Electronics and Control Techniques for Maximum Energy Harvesting in Photovoltaic Systems. Boca Raton, Florida: CRC Press, p7-12.

[8] Pveducation.org. PV Education. [online] Available at: http://www.pveducation.org [March 2017]

[9] Ni.com. (2017). Part II – Photovoltaic Cell I-V Characterization Theory and LabVIEW Analysis Code - National Instruments. [online] Available at: http://www.ni.com/white-paper/7230/en /

[10] Conserve Energy Future. Various Disadvantages of Solar Energy - Conserve Energy Future. [online] Available at: http://www.conserve-energy-future.com/Disadvantages_SolarEnergy.php [April 2017]

[11] Solarpoweristhefuture.com. Problems with Solar Energy. [online] Available at: http://www.solarpoweristhefuture.com/problems-with-solar-energy.shtml [April 2017]

[12] Muenster, R J. (2009). Renewableenergyworld.com. (2017). Shade happens: installation considerations with solar panels. [online] Available at: http://www.renewableenergyworld.com/articles/2009/03/shade-happens-installation.html

[13] Kefif, N. and Belhamici, S. and Kheldoune, A. and Metidji, B. PV Module Parameters Identification Using Datasheet and Experimental Data. Institute of Electrical and Electronic Engineering, University M'Hamed BOUGARA Boumerdes.

[14] Wikipedia. (2004). Arduino. [online] en.wikipedia.org/wiki/Arduino. Available at: https://en.wikipedia.org/wiki/Arduino

[15] Arduino.cc. Arduino - Home. [online] Available at: https://www.arduino.cc [May 2017]

[16] Hejri, M. Mokhtari, H. Azizian, MR. Soder, L. (2013). An Analytical-numerical Approach for Parameter Determination of a Five-parameter Single-diode Model of Photovoltaic Cells and Modules. International Journal of Sustainable Energy, 35(4), pp.396-410.

[17] Wikipedia. (2004). Global Optimization. [online] en.wikipedia.org/wiki/Global_ optimization. Available at: http:// en.wikipedia.org/wiki/Global_optimization [May 2017]

[18] Yang, XS. (2014). Nature Inspired Algorithms. London: Elsevier

[19] Ghorbani, N. Babaei, E. (2014). The Exchange Market Algorithm. Applied Soft Computing, 2014 (19), p177-187.

[20] D.T. Pham, A. Ghanbarzadeh, E. Koç, S. Otri , S. Rahim , M. Zaidi. (2006). The Bees Algorithm – A Novel Tool for Complex Optimisation Problems. Manufacturing Engineering Centre, Cardiff University.

[21] Chen, T. Xiao, R. (2013). Enhancing Artificial Bee Colony Algorithm with Self-Adaptive Searching Strategy and Artificial Immune Network Operators for Global Optimization. The Scientific World Journal, 2014 (6).

Appendices

ENGINEERING DRAWING (mm)

Rear View

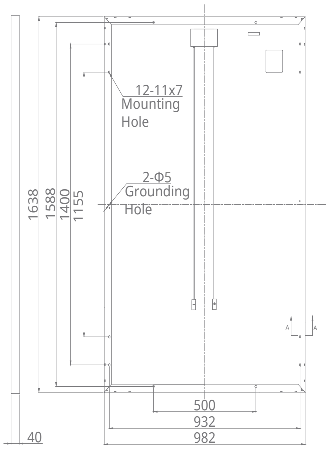

Frame Cross Section A-A

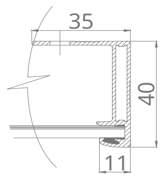

Mounting Hole

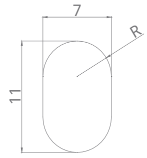

CS6P-265P / I-V CURVES

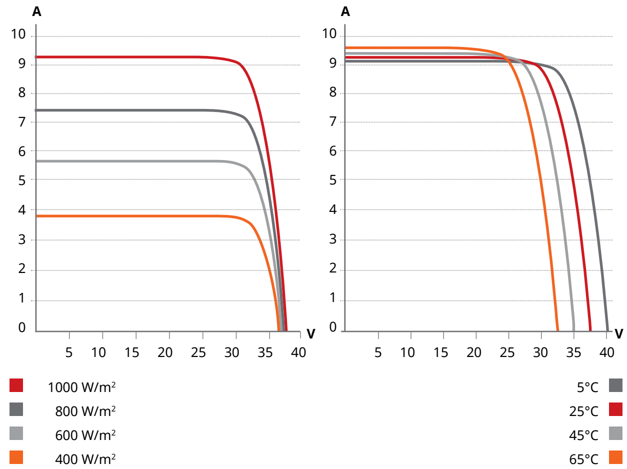

ELECTRICAL DATA | STC*

CS6P	260P	265P	270P
Nominal Max. Power (Pmax)	260 W	265 W	270 W
Opt. Operating Voltage (Vmp)	30.4 V	30.6 V	30.8 V
Opt. Operating Current (Imp)	8.56 A	8.66 A	8.75 A
Open Circuit Voltage (Voc)	37.5 V	37.7 V	37.9 V
Short Circuit Current (Isc)	9.12 A	9.23 A	9.32 A
Module Efficiency	16.16%	16.47%	16.79%
Operating Temperature	-40°C ~ +85°C		
Max. System Voltage	1000 V (IEC) or 1000 V (UL)		
Module Fire Performance	TYPE 1 (UL 1703) or CLASS C (IEC 61730)		
Max. Series Fuse Rating	15 A		
Application Classification	Class A		
Power Tolerance	0 ~ + 5 W		

* Under Standard Test Conditions (STC) of irradiance of 1000 W/m², spectrum AM 1.5 and cell temperature of 25°C.

MECHANICAL DATA

Specification	Data
Cell Type	Poly-crystalline, 6 inch
Cell Arrangement	60 (6×10)
Dimensions	1638×982×40 mm (64.5×38.7×1.57 in)
Weight	18 kg (39.7 lbs)
Front Cover	3.2 mm tempered glass
Frame Material	Anodized aluminium alloy
J-Box	IP67, 3 diodes
Cable	4 mm² (IEC) or 4 mm² & 12 AWG 1000 V (UL), 1000 mm (39.4 in) (650 mm (25.6 in) is optional)
Connectors	T4 series or PV2 series
Per Pallet	26 pieces, 515 kg (1135.4 lbs)
Per Container (40' HQ)	728 pieces

ELECTRICAL DATA | NOCT*

CS6P	260P	265P	270P
Nominal Max. Power (Pmax)	189 W	192 W	196 W
Opt. Operating Voltage (Vmp)	27.7 V	27.9 V	28.1 V
Opt. Operating Current (Imp)	6.80 A	6.88 A	6.97 A
Open Circuit Voltage (Voc)	34.5 V	34.7 V	34.8 V
Short Circuit Current (Isc)	7.39 A	7.48 A	7.55 A

* Under Nominal Operating Cell Temperature (NOCT), irradiance of 800 W/m², spectrum AM 1.5, ambient temperature 20°C, wind speed 1 m/s.

TEMPERATURE CHARACTERISTICS

Specification	Data
Temperature Coefficient (Pmax)	-0.41 % / °C
Temperature Coefficient (Voc)	-0.31 % / °C
Temperature Coefficient (Isc)	0.053 % / °C
Nominal Operating Cell Temperature	45±2 °C

PERFORMANCE AT LOW IRRADIANCE

Outstanding performance at low irradiance, with an average relative efficiency of 96.5 % from irradiances, between 1000 W/m² and 200 W/m² (AM 1.5, 25°C).

The specification and key features described in this datasheet may deviate slightly and are not guaranteed. Due to on-going innovation, research and product enhancement, Canadian Solar Inc. reserves the right to make any adjustment to the information described herein at any time without notice. Please always obtain the most recent version of the datasheet which shall be duly incorporated into the binding contract made by the parties governing all transactions related to the purchase and sale of the products described herein.

Caution: For professional use only. The installation and handling of PV modules requires professional skills and should only be performed by qualified professionals. Please read the safety and installation instructions before using the modules.

PARTNER SECTION

Scan this QR-code to discover solar projects built with this module

LDK SOLAR

MONOCRYSTALLINE MODULES

160D-165D-170D-175D-180D-185D-190D-24

ELECTRIC CHARACTERISTICS (STC*)

Type	160D-24	165D-24	170D-24	175D-24	180D-24	185D-24	190D-24
Nominal Output (Pmax) [W]	160	165	170	175	180	185	190
Warranted Minimum Power [W]	155.2	160.05	164.9	169.75	174.6	179.45	184.3
Flash Test Power Classification	0/+5 W	0/+5 W	0/+5 W	0/+5 W	0/+5 W	0/+5 W	0/+5 W
Voltage at Pmax (Vmp) [V]	35.0	35.2	35.4	35.9	36.2	36.9	37.7
Current at Pmax (Imp) [A]	4.6	4.68	4.76	4.87	4.98	5.02	5.05
Open Circuit Voltage (Voc) [V]	44.0	44.2	44.5	44.7	44.9	45.1	45.2
Short Circuit Current (Isc) [A]	5.38	5.40	5.42	5.43	5.46	5.48	5.51
Maximum System Voltage	IEC: 1000 V / UL: 600 V						
Maximum Series Fuse Rating	10A						
Cell Efficiency [%]	15.37	15.85	16.33	16.81	17.28	17.77	18.25
Module Efficiency [%]	12.48	12.88	13.27	13.66	14.05	14.44	15.22

STC (Standard Test Conditions): Irradiance 1000W/m², Module Temperature 25°C, Air Mass 1.5*

PERFORMANCE AT LOW IRRADIANCE

The typical relative change in module efficiency at an irradiance of 200W/m² in relation to 1000W/m²(both at 25°C and AM 1.5 spectrum) is less than 6%

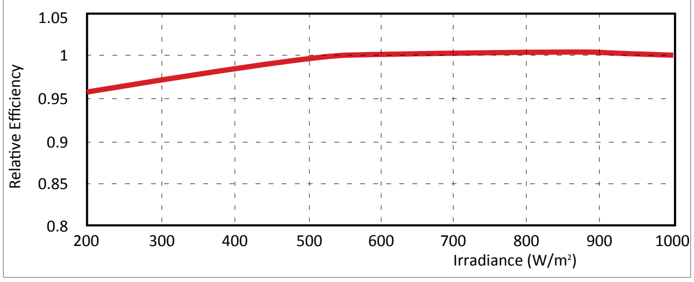

ELECTRICAL PERFORMANCE AT NOCT

Type	160D-24	165D-24	170D-24	175D-24	180D-24	185D-24	190D-24
Nominal Output (Pmax) [W]	116	120	123	127	130	134	138
Voltage at Pmax (Vmp) [V]	29.8	30.7	31.3	32.3	32.8	33.6	34.6
Current at Pmax (Imp) [A]	3.89	3.91	3.93	3.94	3.96	3.98	3.99
Open Circuit Voltage (Voc) [V]	40.5	40.7	41.0	41.2	41.3	41.5	41.6
Short Circuit Current (Isc) [A]	4.36	4.37	4.39	4.40	4.42	4.44	4.46

NOCT: Irradiance 800 W/m², Module Temperature 45± 2 °C, Air Mass 1.5

IV CURVE AT DIFFERENT IRRADIANCE LEVELS

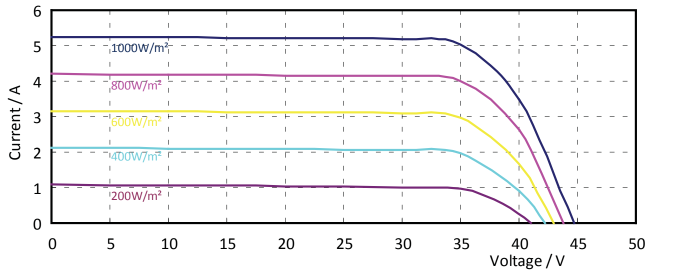

Above graphics according to LDK-175D-24

TEMPERATURE CHARACTERISTICS

Type	LDK-D-24 Series
NOCT**	45±2 °C
Temperature Coefficient of Pmax	-0.47 % / °C
Temperature Coefficient of Voc	-0.34 % / °C
Temperature Coefficient of Isc	0.06 % / °C
Operating Temperature	-40°C to +85°C

*NOCT**: Nominal Operation Cell Temperature Sun 800W/m2; Air 20°C; Wind speed 1m/s*

MECHANICAL CHARACTERISTICS

Type	LDK-D-24 Series
Solar Cells	72(6x12) monocrystalline cells 125mm
Front Cover	3.2mm thick, low iron tempered glass
Back Cover	TPT (Tedlar-PET-Tedlar)
Encapsulant	EVA (Ethylene vinyl acetate)
Frame	Anodized aluminium alloy, double wall
Diodes	6 Bypass diodes serviceable
Junction Box	IP65 rated
Connector	MC4 or compatible connector
Cables	Length: 1200 mm / Section: 4.0 mm²
Dimension	1586 x 808 x 40 mm / 62.4 x 31.8 x 1.6 inches
Weight	15.6 Kg / 34.4 lbs
Max.Load	Certified to 5400Pa

DIMENSIONS

Front View | Back View

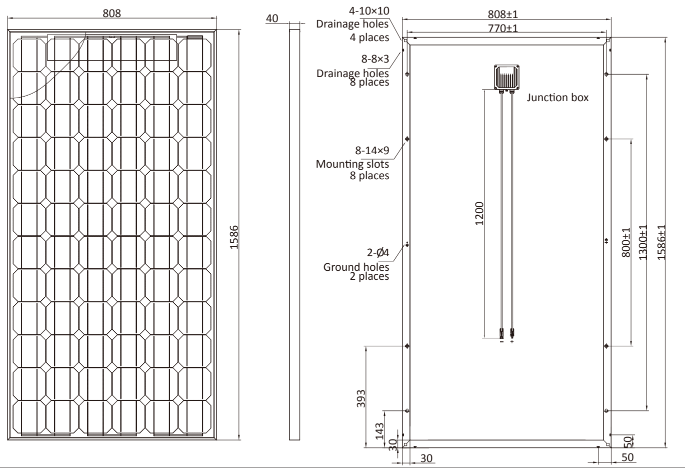

PACKING CONFIGURATION

Type	LDK-D-24 Series
Packing Configuration	24 pcs. / box
Quantity / Pallet	48 pcs. / pallet
Loading Capacity	624 pcs. / 40ft (H)

Partner:

Contact Us:

module.sales@ldksolar.com
www.ldksolar.com

PLM-250P-60 SERIES
Polycrystalline SERIES

PERLIGHT SOLAR
Powering Possibilities

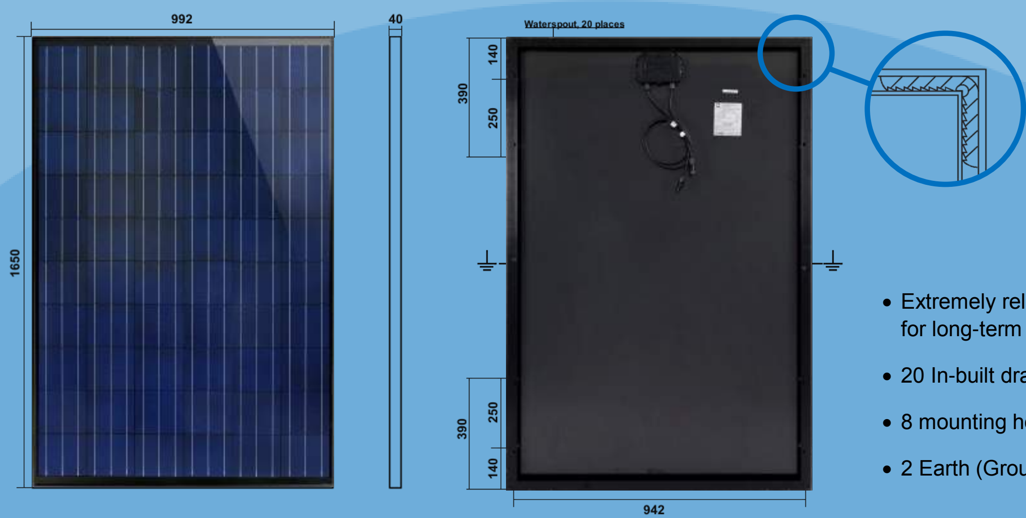

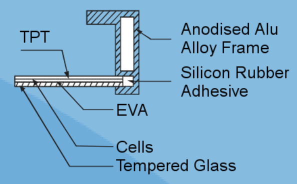

- Extremely reliable screw-less, interconnected frame for long-term flexibility and strength.
- 20 In-built drainage waterspouts.
- 8 mounting holes for direct mounting option.
- 2 Earth (Ground) points.

Module	PLM-250P-60	PLM-255P-60	PLM-260P-60
Pm	**250W**	**255W**	**260W**
Vmp	31.73	31.96	32.10
Imp	7.88	7.98	8.10
Voc	37.58	37.73	37.92
Isc	8.49	8.52	8.64
Cell Efficiency	17.64%	17.99%	18.34%
Module Efficiency	15.27%	15.58%	15.88%
Output per m²	152.74W/m²	155.79W/m²	158.85W/m²

Temperature Coefficient	
NOCT	45ºC+/-2ºC
Isc	0.06%/ºC
Voc	-0.34%/ºC
Pmax	-0.45%/ºC

Power Tolerance	-0/+3%
Working Temperature	-40ºC to 85ºC
Max. System Voltage	1000VDC
Module Area	1.64m²
Wind Rating	5400Pa
Hail Resistance	25mm @ 80km/h
Max. Fuse Rating	15 Amp

Electrical Curves:
PLM-250P-60

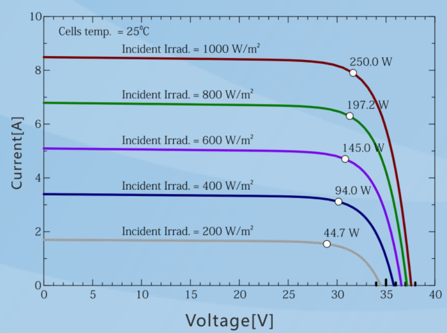

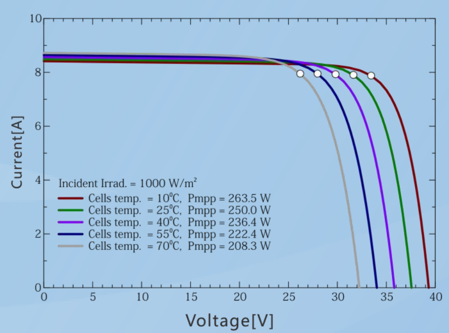

- IEC61730 safety rated for high wind pressure, hail impact, snow load and fire .
- Certified against Salt mist corrosion for coastal areas.
- Certified against Ammonia corrosion for agricultural installations.
- Produced in an environmentally friendly ISO 9001, OHSAS 18001 and ISO 14000 certified manufacturing facility, which has been utilizing an onsite 360kW Perlight Solar system since 2006.

PERLIGHT SOLAR
Powering Possibilities

Available from:

MANUFACTURING BASE
Perlight Solar Co.,Ltd
Muyu Administration District
Wenling
Zhejiang, 317521, China
Tel: +86 576 8647 7290
E: Jenny.uk@perlight.com

GLOBAL MARKETING CENTRE
Perlight Solar Co.,Ltd
E# 14th floor, 58 Xinjinqiao Rd
PuDong District
Shanghai, 200129, China
Tel: +86 21 6105 2372
E: enquiry@perlight.com

EU SALES AND CUSTOMER CENTRE
Westech Solar (UK) Ltd
Unit 1, Bobby Fryer Close,
Garsington Rd
Oxford, OX4 6ZN, UK
Tel: +44 (0)1865 682 584
E: info@westech-solar.co.uk

PERLIGHT westech

2015.06

KD135SX-UPU

ELECTRICAL CHARACTERISTICS

Current-Voltage characteristics of Photovoltaic Module KD135SX-UPU at various cell temperatures

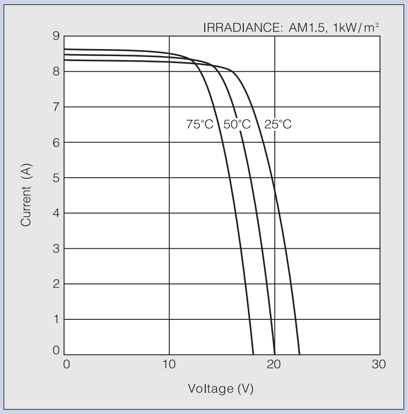

Current-Voltage characteristics of Photovoltaic Module KD135SX-UPU at various irradiance levels

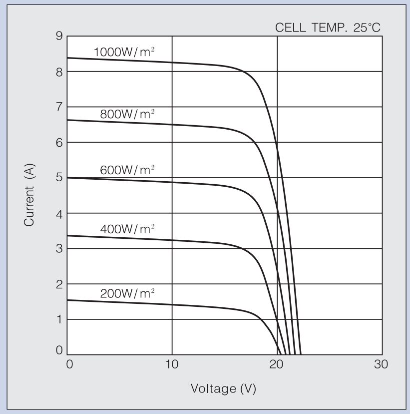

SPECIFICATIONS

■ Physical Specifications

Unit : mm (in)

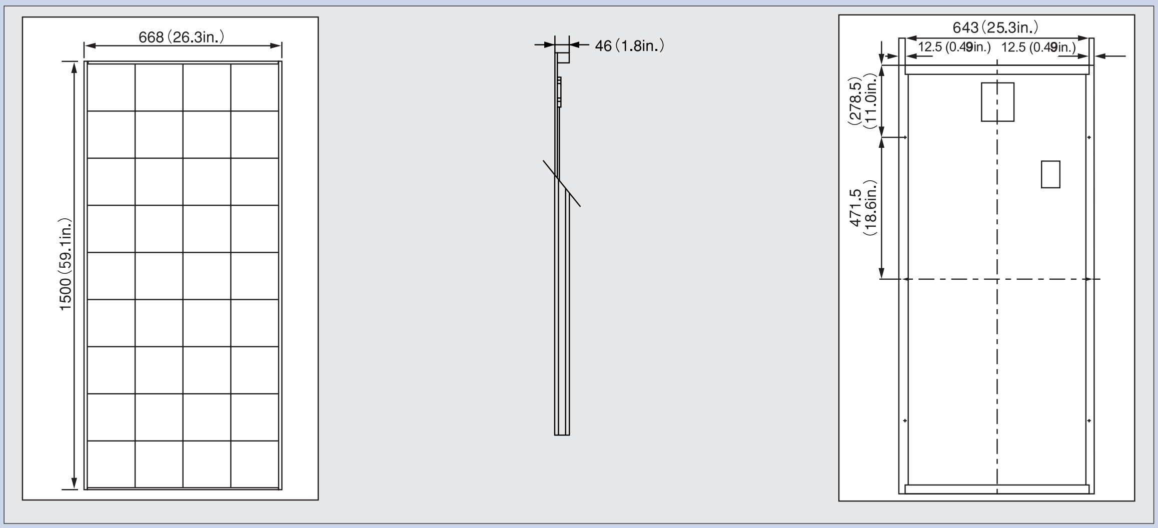

■ Specifications

■ Electrical Perfomance under Standard Test Conditions (*STC)	
Maximum Power (Pmax)	135W (+5%/–5%)
Maximum Power Voltage (Vmpp)	17.7V
Maximum Power Current (Impp)	7.63A
Open Circuit Voltage (Voc)	22.1V
Short Circuit Current (Isc)	8.37A
Max System Voltage	600V
Temperature Coefficient of Voc	-8.0×10^{-2} V/°C
Temperature Coefficient of Isc	5.02×10^{-3} A/°C

*STC : Irradiance 1000W/m², AM1.5 spectrum, cell temperature 25°

■ Electrical Performance at 800W/m², *NOCT, AM1.5	
Maximum Power (Pmax)	95W
Maximum Power Voltage (Vmpp)	15.7V
Maximum Power Current (Impp)	6.10A
Open Circuit Voltage (Voc)	20.0V
Short Circuit Current (Isc)	6.79A

*NOCT (Nominal Operating Cell Temperature) :47.9°C

■ Cells	
Number per Module	36

■ Module Characteristics	
Length x Width x Depth	1500mm(59.1in)x668mm(26.3in)x46mm(1.8in)
Weight	12.5kg(27.5lbs.)

■ Junction Box Characteristics	
Length x Width x Depth	150mm(5.9in)x140mm(5.5in)x37.2mm(1.5in)
IP Code	IP65

■ Others	
*Operating Temperature	–40°~90°C
Maximum Fuse	15A

*This temperature is based on cell temperature.

ISO 9001 and ISO 14001 Certified and Registered

www.kyocerasolar.com
800-223-9580 toll free 800-523-2329 fax

KYOCERA

MECHANICAL SPECIFICATION

Length	1196 (+1/-0.5) mm
Width	636 (+1/-0.5) mm
Height	36 mm (incl. junction box and frame)
Weight	14.5 kg
Front Cover	4 mm tempered low iron glass
Back Cover	3 mm float glass
Frame	Black anodized aluminium
Cell Type	CIGS [Cu(In, Ga) Se_2]
Junction box	Protection class IP 65, with 1 bypass diode (3 A) 66 x 54 x 15 mm³
Cable type	Solar cable 2.5 mm²; (+) 855 (+30/-0) mm; (–) 735 (+30/-0) mm
Connector	MC4

TECHNICAL DRAWING

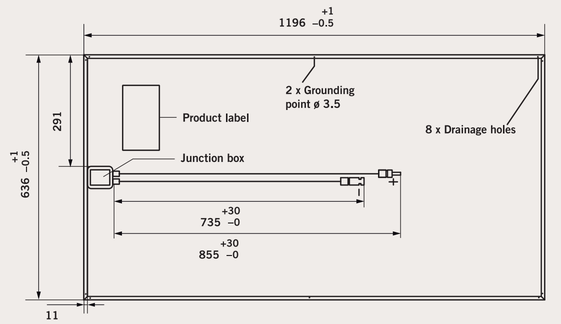

ELECTRICAL CHARACTERISTICS

PERFORMANCE AT STANDARD TEST CONDITIONS (STC: 1000 W/m², 25 °C, AM 1.5 SPECTRUM)[1]

POWER CLASS			75	80	85	90	95
Nominal Power (+5/-0 Wp)	P_{MAX}	[W]	75.0	80.0	85.0	90.0	95.0
Short Circuit Current	I_{SC}	[A]	1.66	1.66	1.67	1.67	1.68
Open Circuit Voltage	V_{OC}	[V]	74.4	74.5	75.2	76.5	78.0
Current at Maximum Power	I_{MPP}	[A]	1.40	1.42	1.44	1.48	1.53
Voltage at Maximum Power	V_{MPP}	[V]	53.6	56.4	59.0	60.8	62.1
Nominal Efficiency	η	[%]	≥9.9	≥10.5	≥11.2	≥11.8	≥12.5

PERFORMANCE AT NORMAL OPERATING CELL TEMPERATURE (NOCT: 800 W/m², 51 ±2 °C, AM 1.5 SPECTRUM)

POWER CLASS			75	80	85	90	95
Nominal Power	P_{MAX}	[W]	54.2	57.8	61.4	65.1	68.7
Short Circuit Current	I_{SC}	[A]	1.33	1.33	1.33	1.33	1.34
Open Circuit Voltage	V_{OC}	[V]	67.7	67.8	68.4	69.6	71.0
Current at Maximum Power	I_{MPP}	[A]	1.11	1.13	1.14	1.18	1.22
Voltage at Maximum Power	V_{MPP}	[V]	48.6	51.2	53.5	55.2	56.3

[1] Measurement accuracy: ±10 %. All STC measurements based on pre-treatement of modules with 1 hour light soak (1000 W/m² [1 kWh/m²], in open circuit) followed by cool down to 25 °C. For the system conception, please take into account the typical relative V_{OC} and V_{MPP} power increase of 2.5 % after 215 kWh/m² light soaking. This power boost is not included in the nominal values of this data sheet.

PERFORMANCE AT LOW IRRADIANCE

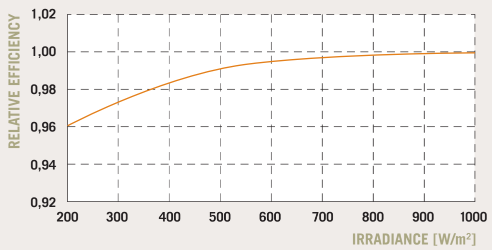

The typical relative change in module efficiency (at nominal power) at an irradiance of 200 W/m² in relation to 1000 W/m² (both at 25 °C and AM 1.5 spectrum) is -4.0 % rel.

CHARACTERISTICS AT DIFFERENT TEMPERATURES AND IRRADIANCES

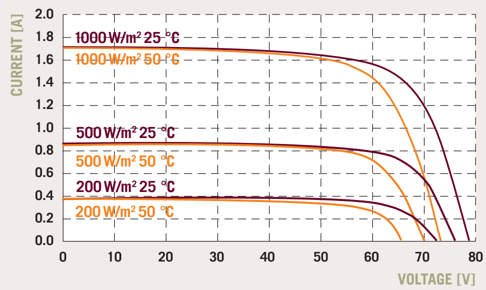

TEMPERATURE COEFFICIENTS (AT 1000 W/m², AM 1.5 SPECTRUM)

Temperature Coefficient of I_{SC}	α	[%/K]	+ 0.00 ±0.04	**Temperature Coefficient of V_{OC}**	β	[%/K]	–0.29 ±0.04
Temperature Coefficient of P_{MAX}	γ	[%/K]	–0.38 ±0.04				

PROPERTIES FOR SYSTEM DESIGN

Maximum System Voltage V_{SYS}	[V]	1000 (IEC) / 600 (UL 1703)	**Safety Class**	II
Maximum Reverse Current I_R	[A]	5.1	**Fire Rating**	C
Wind/Snow Load	[Pa]	5400	**Permitted module temperature on continous duty**	-40 °C up to +85 °C

QUALIFICATIONS AND CERTIFICATES

IEC 61646 (Ed. 2), IEC 61730 (Ed.1) application class A, UL 1703
The production site is certified according to ISO 9001 for Quality Management.

Safety Class II

C Certified UL 1703 US

The content of this data sheet is according to DIN EN 50380.

PARTNER

NOTE: Installation instructions must be followed. See the installation and operating manual or contact the technical service for further information on approved installation and use of this product.

Q-CELLS SE
OT Thalheim, Sonnenallee 17–21
06766 Bitterfeld-Wolfen, Germany

TEL +49 (0)3494 66 99-0
FAX +49 (0)3494 66 99-199

EMAIL service@q-cells.com
WEB www.q-cells.com

Mechanical data

Cell	Monocrystalline (156.5 mm)² silicon solar cells
Quantity and wiring of cells	48 in series
Dimensions	1,318 × 994 × 46 mm (1.31 m²)
Weight	16 kg
Connection type	Cable with plug connector (MC-3)

Limit values

Operating temperature (cell) Storage temperature	– 40 to + 90	°C
Storage air humidity (relative)	up to 90	%
Maximum system voltage	1,000	V DC
Maximum mechanical load	2,400	N/m²
Over-current protection	15	A

Electrical data

		NU-185 (E1) NU-S5 (E3E)	NU-180 (E1) NU-S0 (E3E)	
Maximum power	P_{max}	185 W_p	180 W_p	
Open-circuit voltage	V_{oc}	30.2	30.0	V
Short-circuit current	I_{sc}	8.54	8.37	A
Voltage at point of maximum power	V_{mpp}	24.0	23.7	V
Current at point of maximum power	I_{mpp}	7.71	7.6	A
Module efficiency	η_m	14.1	13.7	%
NOCT		47.5	47.5	°C
Temperature coefficient – open-circuit voltage	αV_{oc}	– 104	– 104	mV / °C
Temperature coefficient – short-circuit current	αI_{sc}	+0.053	+0.053	% / °C
Temperature coefficient – power	αP_{max}	– 0.485	– 0.485	% / °C

The electrical data applies under standard test conditions (STCs): irradiation 1,000 W/m² with light spectrum AM 1.5 and a cell temperature of 25 °C. The rated electrical characteristics are subject to a manufacturing tolerance of – 5% / + 10%. NOCT conditions: irradiation of 800 W/m², ambient temperature of 20 °C and wind speed of 1 m/sec.

Characteristic curves NU-180 (E1)

Characteristic curves: current / power vs. voltage (cell temperature: 25 °C)

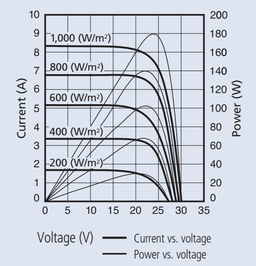

Characteristic curves: open-circuit voltage / short-circuit current vs. irradiation (cell temperature: 25 °C)

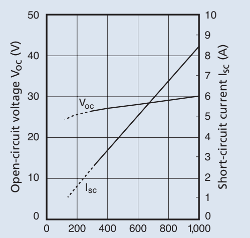

Characteristic curves: normalised values I_{sc} / V_{oc} / P_{max} vs. cell temperature

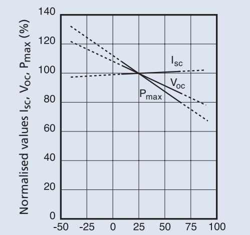

Applications

- On-grid PV systems
- Off-grid PV systems
- On-roof PV systems
- Ground-mounted PV systems

Please read our detailed installation manual carefully before installing the photovoltaic modules.

Exterior dimensions

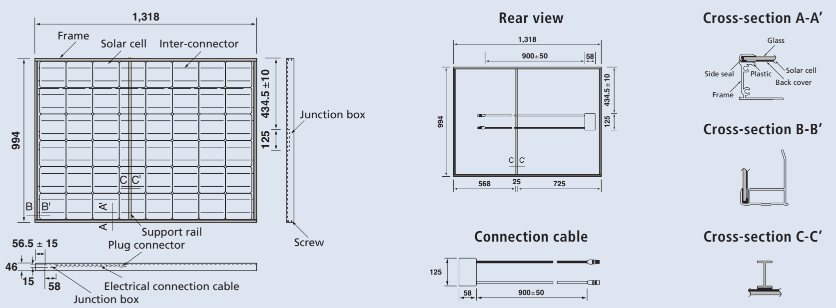

Note

Technical data is subject to change without prior notice. Before using Sharp products, please request the latest data sheets from Sharp. Sharp accepts no responsibility for damage to devices which have been equipped with Sharp products on the basis of unverified information.

The specifications may deviate slightly and are not guaranteed. Installation and operating instructions are to be found in the corresponding handbooks, or can be downloaded from **www.sharp.eu.**

This module should not be directly connected to a load.

Sharp Energy Solution Europe
a division of Sharp Electronics (Europe) GmbH
Sonninstrasse 3, 20097 Hamburg, Germany
Tel: + 49 (0) 40 / 23 76 - 0 • Fax: + 49 (0) 40 / 23 76 - 21 93
www.sharp.eu

Local responsibility:

Austria SolarInfo.at@sharp.eu
Benelux SolarInfo.seb@sharp.eu
Central & Eastern Europe SolarInfo.scee@sharp.eu
Denmark SolarInfo.dk@sharp.eu
France SolarInfo.fr@sharp.eu
Germany SolarInfo.de@sharp.eu
Scandinavia SolarInfo.sen@sharp.eu
Spain & Portugal SolarInfo.es@sharp.eu
Switzerland SolarInfo.ch@sharp.eu
United Kingdom SolarInfo.uk@sharp.eu

SHARP

The reference image on the front page shows a 12.6 kWp system of Osmer-Solartechnik in Grasberg, Germany.

SolarNU_48_E0210

Electrical Characteristics[1]

	BP MSX 60	BP MSX 64[4]
Maximum power (P_{max})[2]	60W	64W
Voltage at P_{max} (V_{mp})	17.1V	17.5V
Current at P_{max} (I_{mp})	3.5A	3.66A
Minimum P_{max}	58W	62W
Short-circuit current (I_{sc})	3.8A	4.0A
Open-circuit voltage (V_{oc})	21.1V	21.3V
Temperature coefficient of I_{sc}	(0.065±0.015)%/°C	
Temperature coefficient of V_{oc}	-(80±10)mV/°C	
Temperature coefficient of power	-(0.5±0.05)%/°C	
NOCT[3]	47±2°C	
Maximum system voltage	600V (U.S. NEC rating) 1000V (TÜV Rheinland rating)	
Maximum series fuse rating	20A	

Notes

1. These data represent the performance of typical MSX 60 and MSX 64 modules as measured at their output terminals, and do not include the effect of such additional equipment as diodes or cables. The data are based on measurements made in accordance with ASTM E1036 corrected to SRC (Standard Reporting Conditions, also known as STC or Standard Test Conditions), which are:
   - illumination of 1 kW/m^2 (1 sun) at spectral distribution of AM 1.5 (ASTM E892 global spectral irradiance);
   - cell temperature of 25°C.
2. During the stabilization process which occurs during the first few months of deployment, module power may decrease approximately 3% from typical P_{max}.
3. The cells in an illuminated module operate hotter than the ambient temperature. NOCT (Nominal Operating Cell Temperature) is an indicator of this temperature differential, and is the cell temperature under Standard Operating Conditions: ambient temperature of 20°C, solar irradiation of 0.8 kW/m^2, and wind speed of 1 m/s.
4. The power of solar cells varies in the normal course of production; the MSX 64 is assembled in limited quantities using cells of slightly higher power than the MSX 60.

MSX 60 I-V Curves

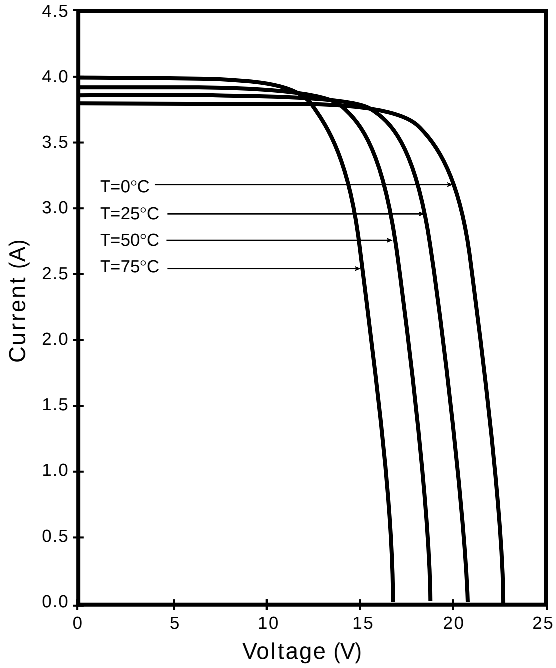

MSX 64 I-V Curves

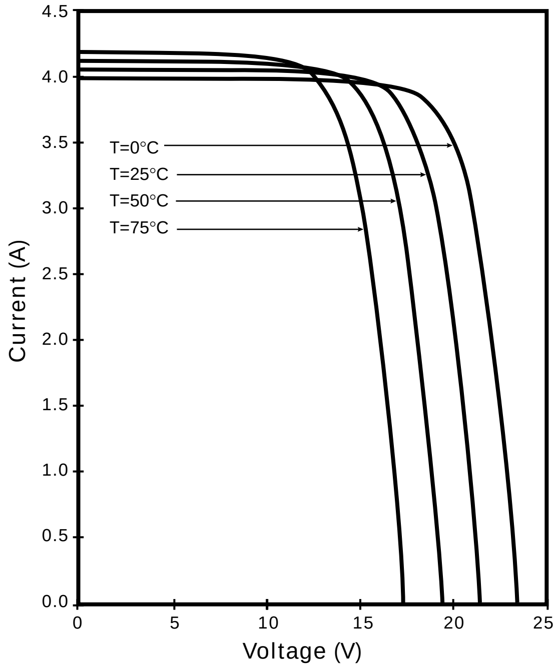

E19 / 240 SOLAR PANEL

SUNPOWER™

MAXIMUM EFFICIENCY AND PERFORMANCE

Electrical Data

Measured at Standard Test Conditions (STC): irradiance of 1000W/m², AM 1.5, and cell temperature 25° C

Peak Power (+5/-3%)	P_{max}	240 W
Efficiency	η	19.3 %
Rated Voltage	V_{mpp}	40.5 V
Rated Current	I_{mpp}	5.93 A
Open Circuit Voltage	V_{oc}	48.6 V
Short Circuit Current	I_{sc}	6.30 A
Maximum System Voltage	UL	600 V
Temperature Coefficients	Power (P)	-0.38% / K
	Voltage (V_{oc})	-132.5mV / K
	Current (I_{sc})	3.5mA / K
NOCT		45° C +/-2° C
Series Fuse Rating		20 A

I-V Curve

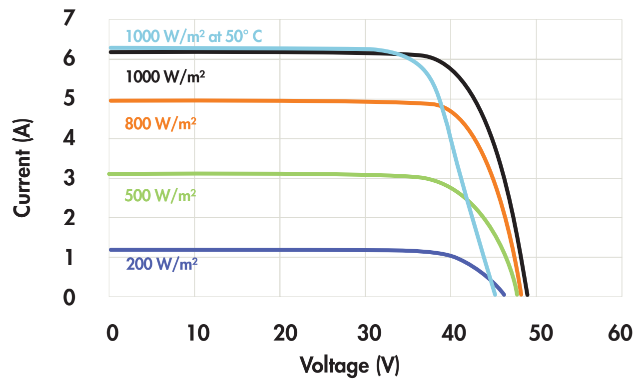

Current/voltage characteristics with dependence on irradiance and module temperature.

Mechanical Data

Solar Cells	72 SunPower all-back contact monocrystalline
Front Glass	High transmission tempered glass with anti-reflective (AR) coating
Junction Box	IP-65 rated with 3 bypass diodes Dimensions: 32 x 155 x 128 (mm)
Output Cables	1000mm length cables / MultiContact (MC4) connectors
Frame	Anodized aluminum alloy type 6063 (black)
Weight	33.1 lbs. (15.0 kg)

Tested Operating Conditions

Temperature	-40° F to +185° F (-40° C to + 85° C)
Max load	113 psf 550kg/m² (5400 Pa) front – e.g. snow; 50 psf 245kg/m² (2400 Pa) front and back – e.g. wind
Impact Resistance	Hail 1 in (25 mm) at 52mph (23 m/s)

Warranties and Certifications

Warranties	25 year limited power warranty
	10 year limited product warranty
Certifications	Tested to UL 1703. Class C Fire Rating

Dimensions

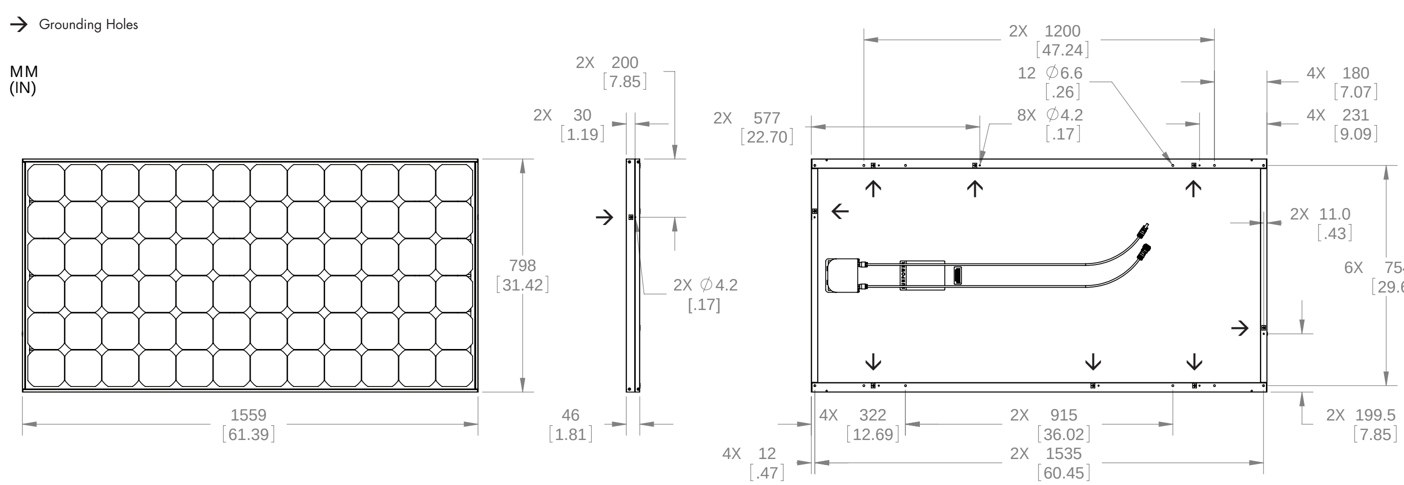

CAUTION: READ SAFETY AND INSTALLATION INSTRUCTIONS BEFORE USING THE PRODUCT.

Visit sunpowercorp.com for details

SUNTECH www.suntech-power.com **Email:** sales@suntech-power.com

	SPECIFICATION CATEGORIES	Db Mono STP005B -12/DEA	Kb Poly STP010D -12/KEA	Cb Mono STP020B -12/CEA	Lb Poly STP030D -12/LEA	Rb Poly STP040D -12/REA	Rb Poly STP045D -12/REA	Md Poly STP050D -12/MEA	Md Poly STP055D -12/MEA
ELECTRICAL CHARACTERISTICS	Open-Circuit Voltage (Voc)	21.6 V	21.6 V	21.7 V	21.6 V	21.8 V	22.0 V	21.8 V	22.2 V
	Optimum Operating Voltage (Vmp)	17.4 V	17.4 V	17.6 V	17.2 V	17.4 V	17.6 V	17.4 V	17.5 V
	Short-Circuit Current (Isc)	0.32 A	0.65 A	1.26 A	1.94 A	2.58 A	2.79 A	3.13 A	3.34 A
	Optimum Operating Current (Imp)	0.29 A	0.57 A	1.14 A	1.74 A	2.30 A	2.58 A	2.93 A	3.14 A
	Maximum Power at STC (Pmax)	5 Wp	10 Wp	20 Wp	30 Wp	40 Wp	45 Wp	50 Wp	55 Wp
	Operating Temperature	-40°C to +85°C	-40°C to +85°C	-40°C to +85°C	-40°C to +85°C	-40°C to +85°C	-40°C to +85°C	-40°C to +85°C	-40°C to +85°C
	Maximum System Voltage	715 V DC	715 V DC	715 V DC	715 V DC	715 V DC	715 V DC	715 V DC	715 V DC
	Maximum Series Fuse Rating	5 A	5 A	5 A	5 A	10 A	10 A	10 A	10 A
	Power Tolerance	±10 %	±10 %	±10 %	±10 %	±5 %	±5 %	±5 %	±5 %
MECHANICAL CHARACTERISTICS	Solar Cell	Mono-crystalline solar cell	Poly-crystalline solar cell	Mono-crystalline solar cell	Poly-crystalline solar cell	Poly-crystalline solar cell	Poly-crystalline solar cell	Poly-crystalline solar cell	Poly-crystalline solar cell
	No. of Cells	36 (4×9)	36 (6×6)	36 (2×18)	36 (4×9)	36 (4×9)	36 (4×9)	36 (4×9)	36 (4×9)
	Dimensions	216 × 306 × 18 mm	310 × 368 × 18 mm	656 × 306 × 18 mm	426 × 680 × 18 mm	537 × 665 × 30 mm	537 × 665 × 30 mm	631 × 665 × 30 mm	631 × 665 × 30 mm
	Weight	0.8 kgs	1.5 kgs	2.5 kgs	3.2 kgs	4.5 kgs	4.5 kgs	6.4 kgs	6.4 kgs
	Junction Box	IP65 rated	IP65 rated	IP65 rated	IP65 rated	IP65 rated	IP65 rated	IP65 rated	IP65 rated
	Output Cables	(Optional cable available)	(Optional cable available)	(Optional cable available)	(Optional cable available)	(Optional cable available)	(Optional cable available)	(Optional cable available)	(Optional cable available)
TEMP. CHARACTERISTICS	Nominal Operating Cell Temperature (NOCT)	45±2°C	45±2°C	45±2°C	45±2°C	45±2°C	45±2°C	45±2°C	45±2°C
	Temp. coefficient of Pmax	-0.48 %/°C	-0.47 %/°C	-0.48 %/°C	-0.47 %/°C	-0.48 %/°C	-0.48 %/°C	-0.47 %/°C	-0.47 %/°C
	Temp. coefficient of Voc	-0.34 %/°C	-0.34 %/°C	-0.34 %/°C	-0.34 %/°C	-0.34 %/°C	-0.34 %/°C	-0.34 %/°C	-0.34 %/°C
	Temp. coefficient of Isc	0.037 %/°C	0.045 %/°C	0.037 %/°C	0.045 %/°C	0.037 %/°C	0.037 %/°C	0.045 %/°C	0.045 %/°C

	SPECIFICATION CATEGORIES	Sb Poly STP060D -12/SEA	Sb Poly STP065D -12/SEA	Sb Poly STP070D -12/SEA	Bb Mono STP080B -12/BEA	Bb Mono STP085B -12/BEA	Tb Poly STP130D -12/TEA	Tb Poly STP135D -12/TEA	Tb Poly STP140D -12/TEA
ELECTRICAL CHARACTERISTICS	Open-Circuit Voltage (Voc)	21.6 V	21.8 V	22.0 V	21.9 V	22.2 V	22.0 V	22.3 V	22.4 V
	Optimum Operating Voltage (Vmp)	17.4 V	17.6 V	17.8 V	17.5 V	17.8 V	17.4 V	17.5 V	17.6 V
	Short-Circuit Current (Isc)	3.90 A	4.11 A	4.27 A	4.95 A	5.15 A	8.09 A	8.20 A	8.33 A
	Optimum Operating Current (Imp)	3.45 A	3.69 A	3.93 A	4.58 A	4.80 A	7.47 A	7.71 A	7.95 A
	Maximum Power at STC (Pmax)	60 Wp	65 Wp	70 Wp	80 Wp	85 Wp	130 Wp	135 Wp	140 Wp
	Operating Temperature	-40°C to +85°C	-40°C to +85°C	-40°C to +85°C	-40°C to +85°C	-40°C to +85°C	-40°C to +85°C	-40°C to +85°C	-40°C to +85°C
	Maximum System Voltage	715 V DC	715 V DC	715 V DC	715 V DC	715 V DC	1000 V DC	1000 V DC	1000 V DC
	Maximum Series Fuse Rating	15 A	15 A	15 A	15 A	15 A	20 A	20 A	20 A
	Power Tolerance	±5 %	±5 %	±5 %	±5 %	±5 %	±5 %	±5 %	±5 %
MECHANICAL CHARACTERISTICS	Solar Cell	Poly-crystalline solar cell	Poly-crystalline solar cell	Poly-crystalline solar cell	Mono-crystalline solar cell	Mono-crystalline solar cell	Poly-crystalline solar cell	Poly-crystalline solar cell	Poly-crystalline solar cell
	No. of Cells	36 (4×9)	36 (4×9)	36 (4×9)	36 (4×9)	36 (4×9)	36 (4×9)	36 (4×9)	36 (4×9)
	Dimensions	771 × 665 × 30 mm	771 × 665 × 30 mm	771 × 665 × 30 mm	1195 × 541 × 30 mm	1195 × 541 × 30 mm	1482 × 676 × 35 mm	1482 × 676 × 35 mm	1482 × 676 × 35 mm
	Weight	6.2 kgs	6.2 kgs	6.2 kgs	8.0 kgs	8.0 kgs	12.0 kgs	12.0 kgs	12.0 kgs
	Junction Box	IP65 rated	IP65 rated	IP65 rated	IP65 rated	IP65 rated	IP65 rated	IP65 rated	IP65 rated
	Output Cables	H+S (12 AWG) Lengths: 750mm(-) and 750mm(+) Connection: MC Plug Type IV	H+S (12 AWG) Lengths: 750mm(-) and 750mm(+) Connection: MC Plug Type IV	H+S (12 AWG) Lengths: 750mm(-) and 750mm(+) Connection: MC Plug Type IV	H+S (12 AWG) Lengths: 750mm(-) and 750mm(+) Connection: MC Plug Type IV	H+S (12 AWG) Lengths: 750mm(-) and 750mm(+) Connection: MC Plug Type IV	H+S (12 AWG) Lengths: 750mm(-) and 750mm(+) Connection: MC Plug Type IV	H+S (12 AWG) Lengths: 750mm(-) and 750mm(+) Connection: MC Plug Type IV	H+S (12 AWG) Lengths: 750mm(-) and 750mm(+) Connection: MC Plug Type IV
TEMP. CHARACTERISTICS	Nominal Operating Cell Temperature (NOCT)	45±2°C	45±2°C	45±2°C	45±2°C	45±2°C	45±2°C	45±2°C	45±2°C
	Temp. coefficient of Pmax	-0.47 %/°C	-0.47 %/°C	-0.47 %/°C	-0.48 %/°C	-0.48 %/°C	-0.47 %/°C	-0.47 %/°C	-0.47 %/°C
	Temp. coefficient of Voc	-0.34 %/°C	-0.34 %/°C	-0.34 %/°C	-0.34 %/°C	-0.34 %/°C	-0.34 %/°C	-0.34 %/°C	-0.34 %/°C
	Temp. coefficient of Isc	0.045 %/°C	0.045 %/°C	0.045 %/°C	0.037 %/°C	0.037 %/°C	0.045 %/°C	0.045 %/°C	0.045 %/°C

YL 185 P-23b / 1310x990 SERIES

ELECTRICAL PARAMETERS

Electrical parameters at STC (1,000 W/m², 25°C, AM 1.5 according to EN 60904-3)

Module type		YL 165 P-23b	YL 170 P-23b	YL 175 P-23b	YL 180 P-23b	YL 185 P-23b
Power output	[W]	165.0	170.0	175.0	180.0	185.0
Power output tolerances	[%]	+/- 3	+/- 3	+/- 3	+/- 3	+/- 3
Module Efficiency	[%]	12.7	13.1	13.5	13.9	14.3
Voltage at Pmax, V_{mpp}	[V]	23.0	23.0	23.0	23.0	23.5
Current at Pmax, I_{mpp}	[A]	7.17	7.39	7.61	7.83	7.87
Open circuit voltage V_{oc}	[V]	29.0	29.0	29.0	29.5	29.5
Short circuit current I_{sc}	[A]	7.90	8.10	8.20	8.30	8.45
Max. system Voltage	[V]			1,000 VDC		

Parameters of the thermal characteristics

NOCT (Nominal Operating Cell Temperature)	[°C]	46 +/- 2
Temperature coefficient beta of I_{sc}	[1/K]	+ 0.0006
Temperature coefficient alpha of V_{oc}	[1/K]	- 0.0037
Temperature coefficient gamma of P_{mpp}	[1/K]	- 0.0045

IV CURVES

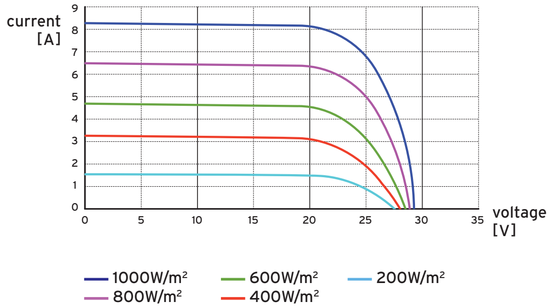

MECHANICAL PARAMETERS

Dimensions (length [mm] / width [mm] / thickness [mm])	1,310 / 990 / 50
Thickness with junction box [mm]	50
Weight [kg]	15.8
Junction box (manufacturer / protection degree / number of diodes)	CIXI / IP65 / 6
Junction box dimensions (length / width / thickness [mm])	151 / 122 / 25
Positive cable & negative cable (manufacturer / length [mm] / cable cross-section [mm²])	CIXI / 900 (1,200) / 4.0
Plug connector (manufacturer / type / protection degree)	MC4 / UV resistance and self-locking / IP67
Front cover (material / thickness [mm])	Tempered Glass, 3.6mm
Cell type (quantity / technology)	48 / polycrystalline / 156 x 156
Encapsulation materials	Ethylene Vinyl Acetate (EVA)
Rear cover (material / thickness [mm])	Le - PET - PVDF / 0.287
Frame (material)	robust anodized aluminum alloy

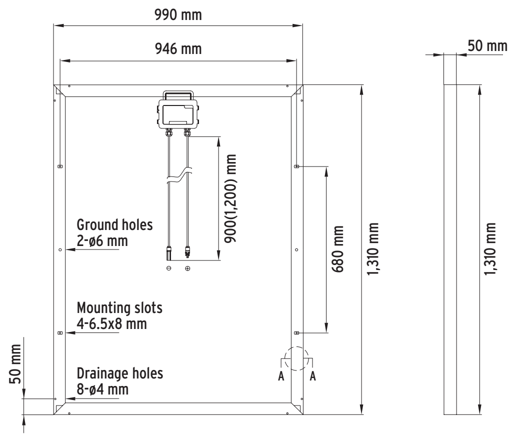

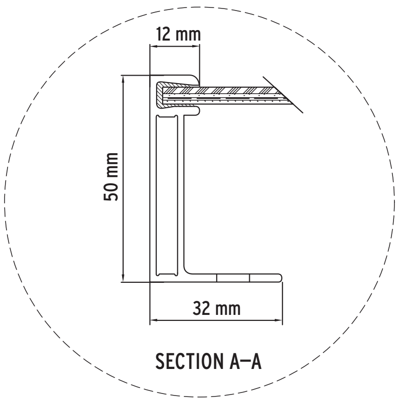

Electrical equipment, check with your installer

www.solar-wind.co.uk

OPERATING CONDITIONS

Operating temperature [°C]	- 40 to + 85
Max. wind load / Max. snow load [Pa]	2.4K / 5.4K

PACKAGING

Number of modules per box	20
Box size (length [mm] / width [mm] / depth [mm])	1,380 / 1,140 / 1,165
Box Gross weight in kg	365
Boxes per pallet	1

* The data does not refer to a single module and they are not part of the offer, they serve for comparison only to different module types.

Yingli Green Energy Holding Co. Ltd.
commerce@yinglisolar.com
0086 - (0)312 - 8929802

Subject to modifications and errors

YINGLI SOLAR
Power Your Life